ELSEVIER

Marine and Petroleum Geology 21 (2004) 555–577

Marine and Petroleum Geology

www.elsevier.com/locate/marpetgeo

Provenance evolution and chemostratigraphy of a Palaeozoic submarine fan-complex: Tanqua Karoo Basin, South Africa

P.O.D. Andersson[a,*], R.H. Worden[b], D.M. Hodgson[b], S. Flint[b]

[a]*Department of Geology and Geochemistry, Stockholm University, S-106 91 Stockholm, Sweden*
[b]*Department of Earth Sciences, University of Liverpool, 4 Brownlow Street, Liverpool L69 3GP, UK*

Received 8 May 2003; received in revised form 6 January 2004; accepted 20 January 2004

Abstract

Geochemical studies of mudstones from boreholes in the deep water Permian Skoorsteenberg Formation in the Karoo Basin of South Africa were undertaken to assess stratigraphic and provenance evolution and the feasibility of chemostratigraphic correlation in this sedimentary setting. Data for 38 major and trace elements including rare earth elements were obtained from four boreholes from 304 samples covering proximal to distal parts of the turbidite complex. There are geochemical signals displaying systematic stratigraphic trends across the basin that imply a continuous evolution of one pre-eminent source terrain that supplied the sediment. Changes in ratios of TiO_2/Al_2O_3, La/(La + Lu) and Th/(Th + Y) suggest an increasingly mafic contribution to the depositional system with time. Perversely, however, increasing Zr and Hf abundance up the stratigraphic succession suggest that there was also an increase in the felsic content with time. These apparently conflicting interpretations may be explained by a single source terrain that became increasingly igneous (e.g. less sedimentary rocks being weathered and supplying new sediment) with time although the progressively denuded rocks must have been predominantly mafic. The chemical index of alteration decreased with time possibly suggesting that a less intense weathering regime in the hinterland developed with time. The geochemical data set from the Skoorsteenberg Formation in the Karoo Basin have demonstrated that chemostratigraphy is not an ideal approach to correlation since the geochemical signals have substantial statistical noise that is not easily related to lithology.

Keywords: Mudstone; Geochemistry; Karoo; Provenance; Chemostratigraphy

1. Introduction

The conventional objective of provenance studies is to reconstruct and interpret the history of sediment supply, from initial erosion of a parent rock to the final burial of its detritus and so to eventually deduce the geographic location and characteristics of the source area. However, the source area of a sedimentary basin is seldom static through time. Under ideal circumstances, changes in the nature of the hinterland can be recognised in the ultimate composition of the sedimentary succession. Important factors such as the location and nature of source area, hinterland drainage pattern and pathways through which sediment has been transferred from source to basin and factors that influence the composition of the sedimentary rocks (e.g. relief, climate, tectonic setting) generally evolve with time. This evolution may be recorded in the characteristics of the sediment that was deposited in the basin (Cox, Lowe, & Cullers, 1995; Davies & Pickering, 1999; Jarvis, Moreton, & Gerard, 1998; Nesbitt, MacRae, & Kronberg, 1990; Nesbitt & Young, 1982; Pearce & Jarvis, 1995; Vital, Stattegger, & Garbe-Schonberg, 1999).

Several studies have documented the viability of bulk elemental analysis in sedimentary provenance studies (Morton, Todd, & Haughton, 1991). Many of the early studies concentrated on the application of major element data (Bhatia, 1983; Roser & Korsch, 1986) however, with significant advances in analytical geochemistry (e.g. ICP-AES, ICP-MS) it is now also possible to reproduce high-quality data for minor and trace elements (see Jarvis and Jarvis (1992a,b) for reviews). Recent studies have emphasized the importance of the relative immobility of certain elements (e.g. REE, Th, Sc, Zr, Y) for the interpretation of

* Corresponding author. Tel.: +46-8-674-78-40; fax: +46-8-674-78-97.
E-mail addresses: daniel.andersson@geo.su.se (P.O.D. Andersson), r.worden@liv.ac.uk (R.H. Worden).

0264-8172/$ - see front matter © 2004 Elsevier Ltd. All rights reserved.
doi:10.1016/j.marpetgeo.2004.01.004

sediment provenance (Davies & Pickering, 1999; Preston et al., 1998; Svendsen & Hartley, 2002).

Correlation of biostratigraphically-barren strata in the sub-surface is difficult and is often achieved based only on broadly similar lithological or petrophysical properties. To improve the stratigraphic resolution of such sections, heavy mineral analyses, palaeomagnetic data and isotope techniques are sometimes applied. An alternative, rapid, and relatively low cost method of performing correlation is chemostratigraphy, or 'chemical stratigraphy'. This technique involves the geochemical characterization and then correlation of strata using major and trace element geochemistry and has been useful when applied to sequences with poor biostratigraphic control (Jarvis et al., 1998; Pearce & Jarvis, 1995; Preston et al., 1998).

In a pilot study of Permian deep-water mudstones of the Skoorsteenberg Formation that crop out in the Tanqua area of the Karoo Basin, Andersson and Worden (in press) applied geochemical and spectral gamma ray techniques. Based on conventional sedimentary logging, two types of mudstones were identified; thick sequences of interfan mudstones that were deposited between sand rich submarine fans and intrafan mudstones which are thinner units deposited between sand layers within each fan. Geochemically-systematic differences between interfan and intrafan mudstones were recorded. The interfan mudstones showed lower SiO_2, TiO_2/Al_2O_3, Zr and Y values than the intrafan mudstones. These differences were interpreted to be controlled by slightly different source lithologies within the same hinterland and changes in relative sea level exposing different parts of the hinterland to erosion and sediment supply. An alternative interpretation involving systematically fluctuating weathering conditions in the hinterland regions was rejected because of seemingly uniform chemical index of alteration (CIA) values for both types of mudstones. The similarity of the rare earth element patterns between the interfan and intrafan mudstones suggested that the two types of mudstones were probably genetically linked and it was unlikely that the two types of mudstone were supplied from radically different landmasses. Stratigraphic trends of TiO_2/Al_2O_3 ratios for both types of mudstones were explained by gradual denudation, exposure and weathering of the different lithologies within the same source area. A relative uranium increase, for both types of mudstones, in the depositional dip direction was recorded from the spectral gamma ray data. The absence of correlation of other uranium-associated characteristics (e.g. total organic carbon) led the authors to interpret this trend as the result of reduced clastic dilution of uranium-bearing pelagic rain into the basin.

The study reported here used core samples of the Skoorsteenberg Formation and aimed to further investigate the inorganic geochemistry of these mudstones as indicators of source area and provenance evolution. Core samples have several advantages over outcrop samples: (1) they have no recent weathering to obscure and pervert the geochemical data, (2) it is easier to obtain a large sample population (note that mudstone is commonly poorly exposed at outcrop), and (3) there is a better overall stratigraphic control (core material provides a continuous record of the stratigraphy) between samples in any given section. A chemostratigraphic approach was also tested to evaluate this technique in comparison to traditional stratigraphic correlation methods.

Four cores from the Tanqua area were sampled for geochemical analyses. The cores were drilled as part of the European Union Framework 5 NOMAD project in order to develop a predictive 3D geological model for deep-water sediments from data collected from the Tanqua submarine fan-complex. In addition to extensive sedimentary logging covering most of the available outcrop and core, comprehensive geological digital data were collected in order to produce detailed correlation panels. Wireline logs and borehole image data (FMI) from the wells were incorporated into the extensive dataset to produce a refined model of the Tanqua submarine fan-complex. There are no biostratigraphic signals with which to correlate the sediments. To improve the stratigraphic control and the prospects for a chemostratigraphic interpretation of the submarine fan-system, a much higher density sampling strategy from the cores was adopted in comparison to the outcrop.

In this paper, we will address four relevant questions inherited from previous geochemical studies on outcrop material.

1. Are there stratigraphic successions with diagnostic geochemical signatures, i.e. 'fingerprints', that are uniform across the submarine fan-system and can be correlated from core to core?
2. How did the provenance of the Skoorsteenberg Formation mudstones evolve through time and what geochemical trace of this evolution can we see in the sedimentary record?
3. How many source terrains were actively supplying sediment to the Tanqua submarine fan-complex?
4. Were different source terrains active during deposition of intrafan mudstones and interfan mudstones?

2. Geological background

The Karoo Basin is a Palaeozoic sedimentary basin (Figs. 1 and 2) developed on top of the Archean Kaapvaal Province, the Kheis Province, the Kibaran Namaqua-Natal Belt and the Pan-African Saldania-Gariep Province (Cole, 1992). The Karoo Basin is generally interpreted to be a foreland basin that formed in front of an advancing thrust and fold belt, the Cape Fold Belt, which wrapped around the southwestern margin of South Africa (Hällbich, 1992; Theron, 1969; Figs. 1 and 2). Following the terminology of Dickinson (1974), the Karoo Basin is a retro-arc foreland basin associated with the formation of the Cape Fold Belt and a magmatic arc south of the fold belt has been inferred (see Johnson (1991)for reviews). The Cape Fold Belt to

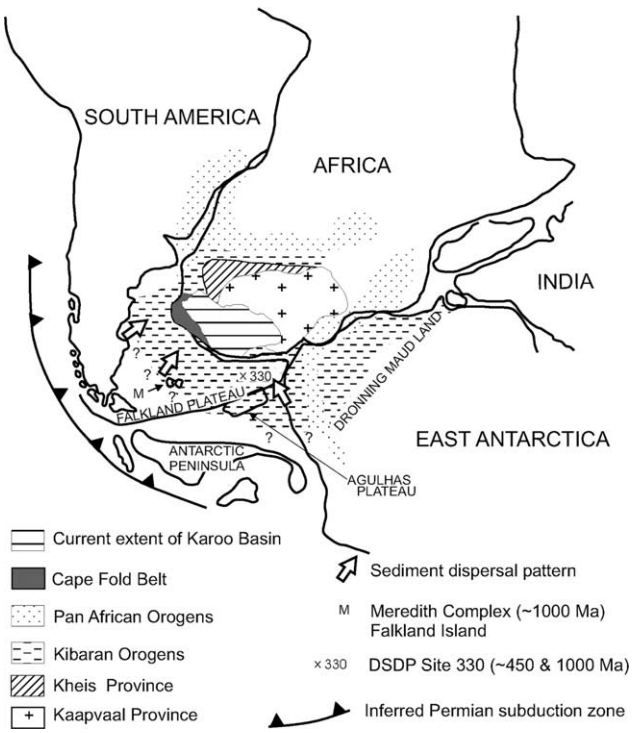

Fig. 1. Location of the Karoo Basin and crustal terranes of South Africa, Antarctica and the Falkland Plateau prior to the break up of Gondwana, modified after De Wit (1977), Duane et al. (1989), Thomas, Agenbacht, Cornell, and Moore (1994).

the south and west of the Karoo Basin contains Neoproterozoic and lower Palaeozoic sedimentary successions and a suite of Pan-African granitoids (Armstrong, de Wit, Reid, York, & Zartman, 1998; Da Silva et al., 2000; Rozendaal, Gresse, Scheepers, & Le Roux, 1999).

The sedimentary fill of the Karoo Basin, the Karoo Supergroup (SACS, 1980), can be divided in the southwestern Karoo basin into the Dwyka Group (Westphalian to

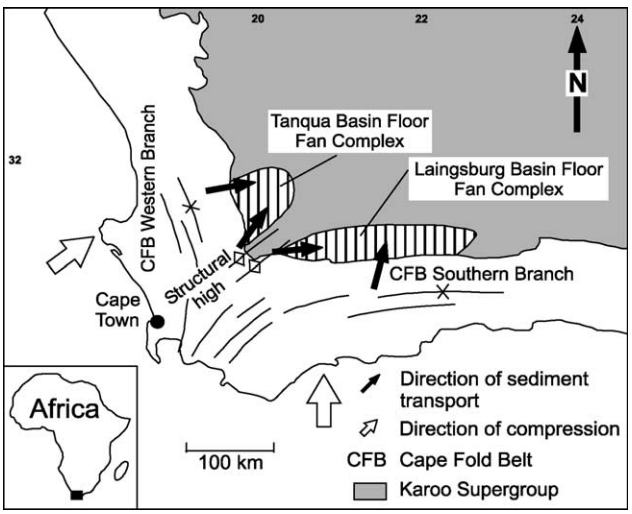

Fig. 2. Location of the Tanqua and Laingsburg basin floor fan-complex in the southwestern corner of the Karoo Basin shown in relation to the two branches of the Cape Fold Belt. (After Wickens, 1992).

early Permian), Ecca Group (Permian) and the Beaufort Group (Permo-Triassic; Fig. 3). The Dwyka Group consists of glacial deposits. Following the Dwyka deglaciation and the concomitant marine transgression, mudstones of the Prince Albert and Whitehill Formations of the Ecca Group were deposited in a large shallow sea that was initially marine but later became brackish (Visser, 1991). The overlying distal turbidites and volcanic ashes of the Collingham Formation provide evidence of active arc volcanism to the south. Mudstones of the Tierberg Formation rest on top of the Collingham Formation and are succeeded by the Skoorsteenberg Formation, the subject of this paper, which contains sand-rich turbidites interbedded with mudstones (Wickens, 1984).

Previous sedimentological outcrop studies of the Skoorsteenberg Formation defined five extensive basin-floor fans in the Tanqua area (Figs. 3 and 4) called informally Fan 1 to Fan 5 from oldest to youngest (Wickens, 1984, 1992). More recent work reinterpreted Fan 5 as a slope fan (Johnson, Flint, Hinds, & Wickens, 2001). Laterally extensive mudstones separate the sandstone-rich basin-floor fans. These interfan mudstones (Fig. 3) have been interpreted to represent times of maximum sediment starvation. The interfan mudstones are thought to be time-correlative with the whole transgressive system tract (TST) and most of the highstand system tract (HST) on the coeval shelf (Johnson et al., 2001), which is not exposed. Basin floor fans 2, 3 and 4 have been interpreted as composite sequences, each composed of several high frequency Exxon-type sequences in which extensive sand-rich 'growth phases' represent lowstand systems tracts (Johnson et al., 2001). Mud-prone units within the fans, here labelled intrafan mudstones, are less laterally extensive than the interfan mudstones and were interpreted by Johnson et al. (2001) as the corresponding TST/HST to the high frequency lowstand systems tracts. Fans 1, 2, 3 and 5 were emplaced in a north-easterly direction based on palaeocurrent data (Johnson et al., 2001; Wickens, 1994), while Fan 4 was interpreted as of westerly derivation (Bouma & Wickens, 1991).

Several authors have suggested that the Cape Fold Belt was the source area for the Ecca and Beaufort Groups of the Karoo Basin (Adelmann & Fiedler, 1998; Cole, 1992; Hälbich, 1983; Kingsley, 1981). This interpretation was challenged by Johnson (1991) who inferred a southern magmatic arc beyond (south of) the Cape Fold Belt as an additional source area for these successions. Electron microprobe studies of heavy minerals in sandstones from the Skoorsteenberg Formation, Vischkuil Formation (equivalent to the Tierberg Formation in the Tanqua area) and Laingsburg Formation by Scott (1997), suggested that the source for these successions also included a high-grade metamorphic terrain. He proposed that this source was located between the magmatic arc on top of the subduction zone and the rising, but still submerged fold-thrust belt.

It is possible that the late Palaeozoic thrust belt was wider than the present Cape Fold Belt. High-grade metamorphic

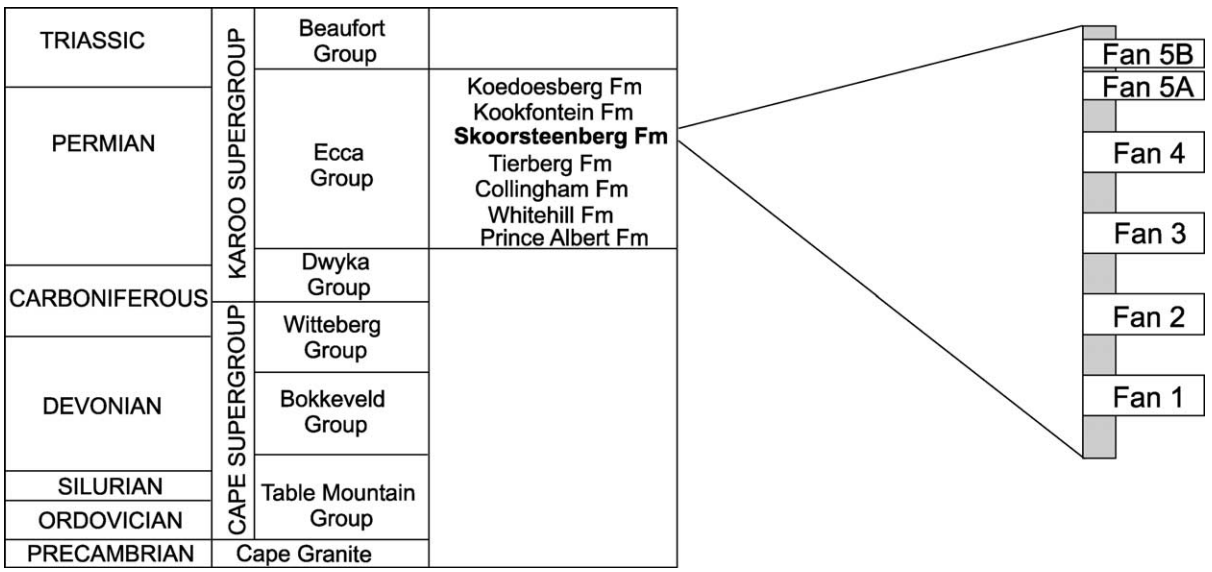

Fig. 3. Stratigraphy of the Cape and Karoo Supergroup in the Western Cape. A schematic stratigraphic log of the Skoorsteenberg Formation submarine fan succession is shown to the right in the figure. Within these fans (Fan 1-5B) are the less extensive intrafan mudstones interlayered while laterally extensive interfan mudstones are deposited between the sand-rich fans (after Bouma & Wickens, 1991).

rocks could have been brought into this belt by reactivation and reverse faulting of the Mesoproterozoic basement, which probably extended more than 100 km south of present-day South Africa (Fig. 1 Beckinsale, Tarney, Darbyshire, & Humm, 1977; De Wit, 1977; Marshall, 1994; Thomas, Jacobs, & Eglington, 2000). Andersson, Johansson, and Kumpulainen (2003) used Sm–Nd data from six sandstone samples from the Skoorsteenberg Formation, representing each of the five submarine fans, to conclude that there was either little or no variation in provenance between the different fans. They suggested that the source areas of the Skoorsteenberg Formation were probably a combination of the late Palaeozoic thrust belt and a contemporaneous magmatic arc to the south that is now not exposed.

Rowsell and De Swardt (1976) suggested that maximum palaeotemperatures in the main Karoo Basin were between 150 and 300 °C from vitrinite reflectance data. Zircon fission track analysis in the southwestern Karoo Basin indicated maximum palaeotemperatures somewhat greater than ~200 °C (Brown, Gallagher, & Duane, 1994). We do not deny the possibility that the mudstones of the Skoorsteenberg Formation may have been affected by later post-depositional diagenetic processes due to the burial history of the Karoo Basin. The diagenetic effects on the mudstones, however, would be similar and relatively symmetrical for the whole studied succession and the geochemical effects comparable. Moreover, the effects of diagenetic alteration on the geochemical signature will be minimal since these are low permeability rocks, thus whatever effects there are will be similar for all the mudstones thus rendering them insignificant.

3. Samples and methods

More than 1300 m of core from four slim boreholes (ns1–4) and three wide boreholes (nb2–4) were recovered

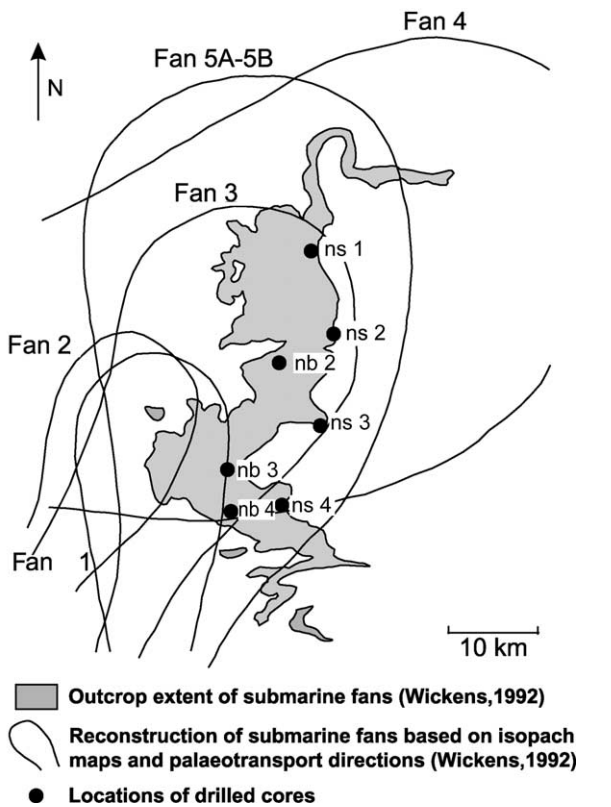

Fig. 4. Reconstruction of the outcrop extent of the Tanqua submarine fans and location of drilled cores (after Wickens, 1992).

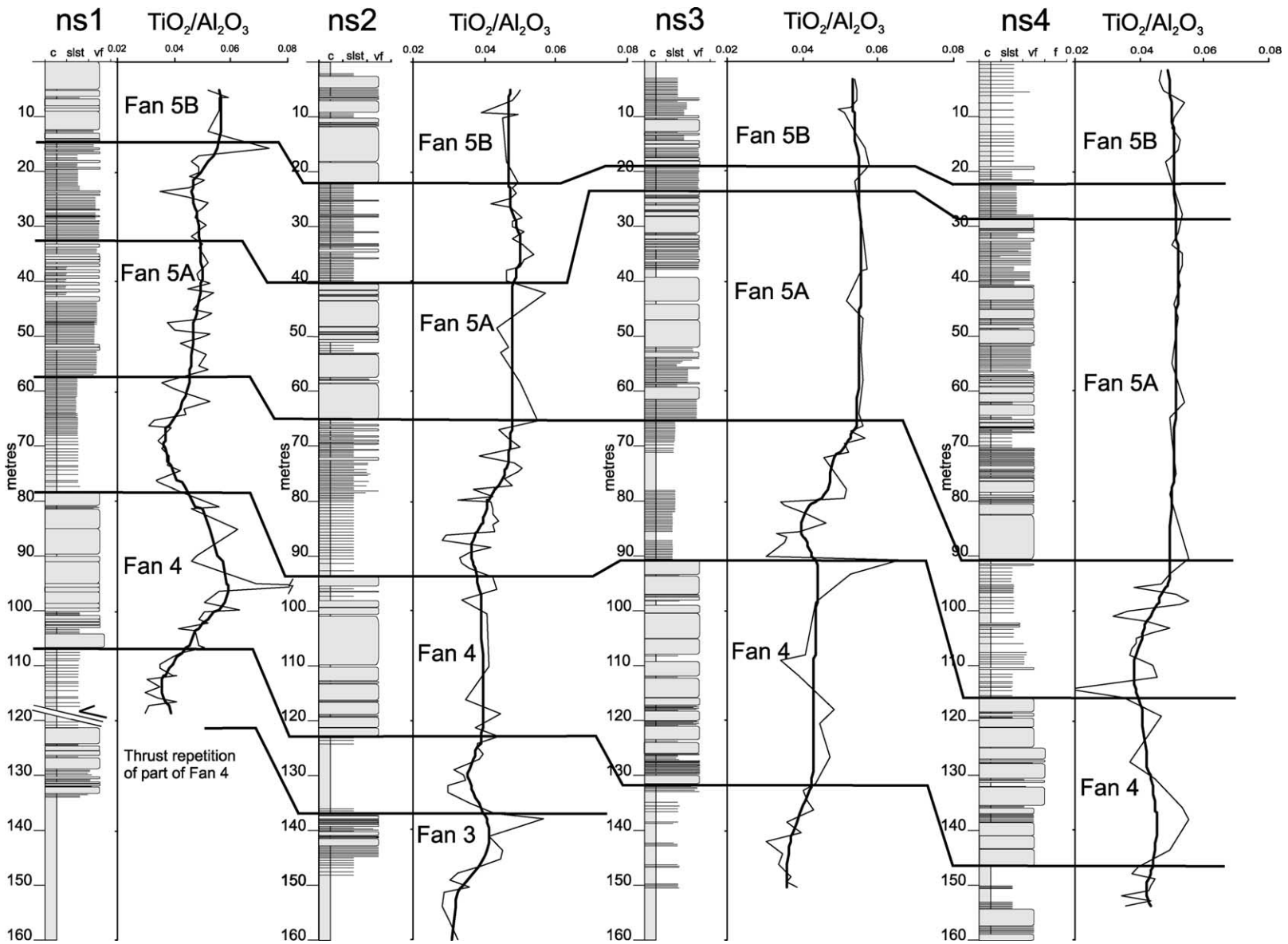

Fig. 5. Chemostratigraphic correlation between core ns1 and ns4 based on TiO_2/Al_2O_3 ratios. Thin lines represent measured element ratios and sample locations are indicated by breaks in the curves. Thick line is recalculated data using a Gaussian running mean filter to produce a smoother average curve. Note the negative peaks in the intervals below Fan 4 and between Fan 4 and Fan 5A in all four cores.

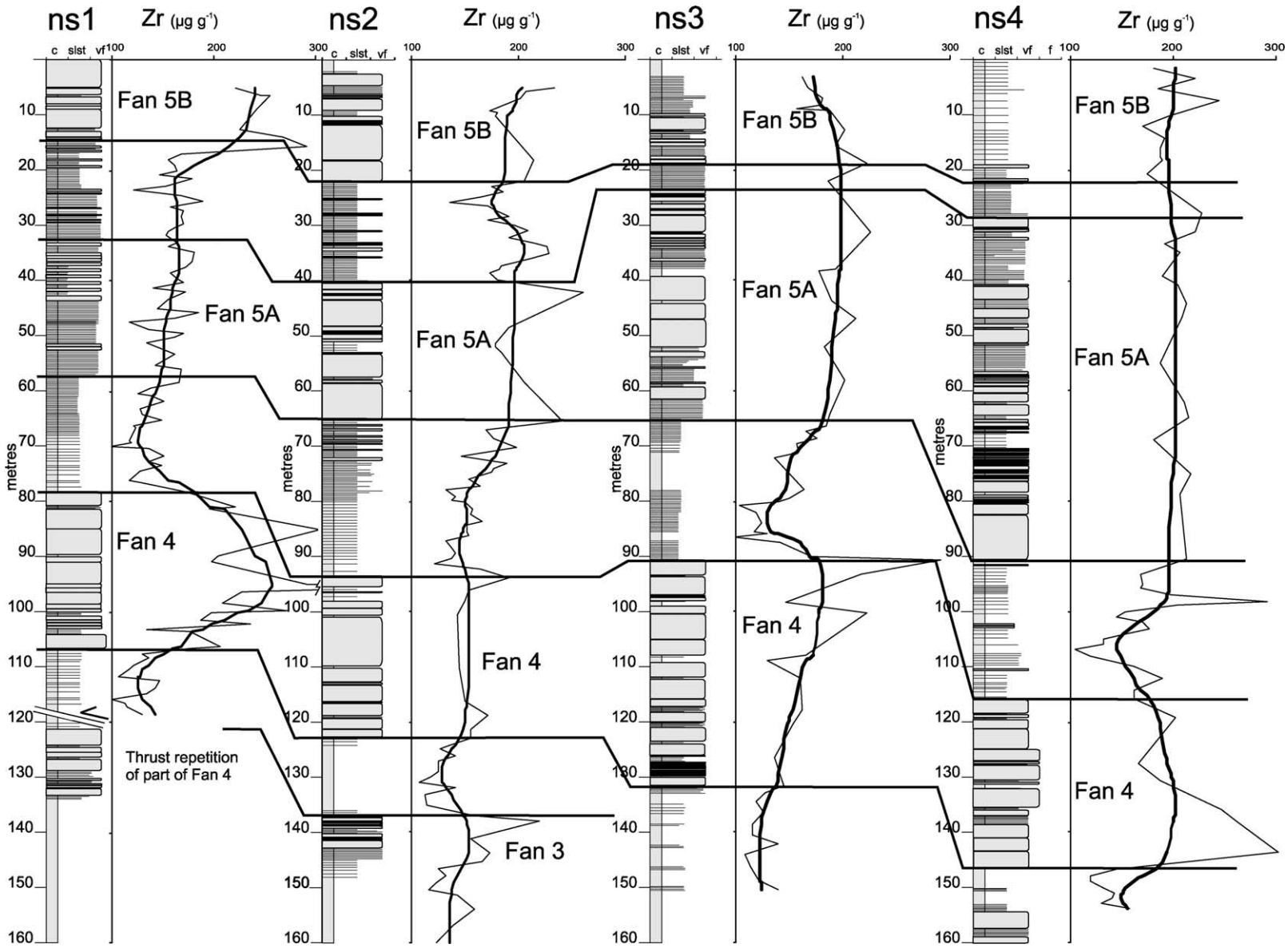

Fig. 6. Chemostratigraphic correlation between core ns1 and ns4 based on Zr data. Thin lines represent measured element ratios and sample locations are indicated by breaks in the curves. Thick line is recalculated data using a Gaussian running mean filter to produce a smoother average curve. Note the negative peaks in the intervals below Fan 4 and between Fan 4 and Fan 5A in all four cores.

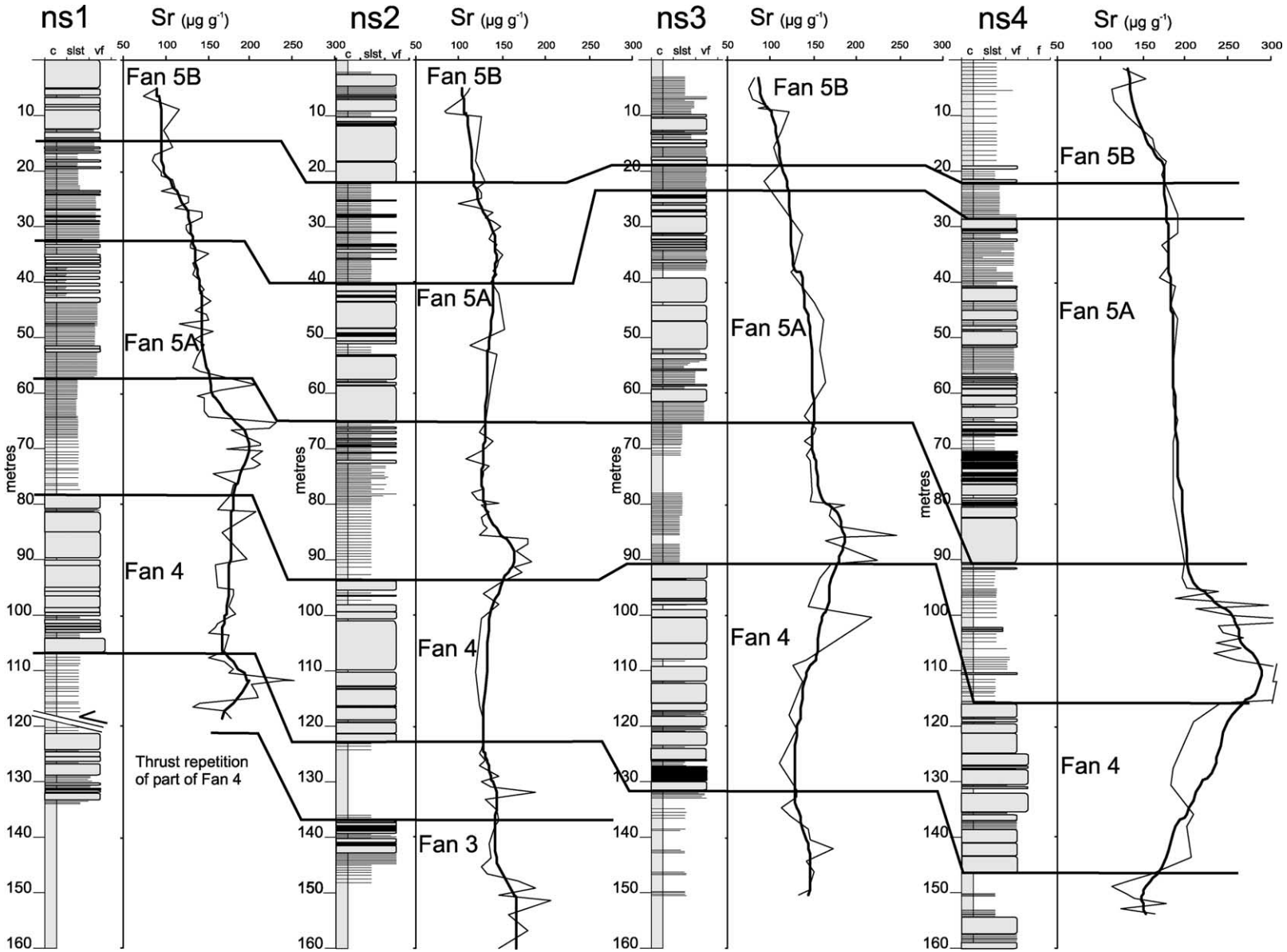

Fig. 7. Chemostratigraphic correlation between core ns1 and ns4 based on Sr data. Thin lines represent measured element ratios and sample locations are indicated by breaks in the curves. Thick line is recalculated data using a Gaussian running mean filter to produce a smoother average curve. Note the positive peak in the interval between Fan 4 and Fan 5A and the general decrease in Sr content from base of Fan 5A and up the stratigraphy in all four cores.

from the Skoorsteenberg Formation (Fig. 4). The drill locations were designed to optimise examination of the sedimentary architecture and geometries of the fans. Recent and ongoing work within the NOMAD project (Hodgson et al., in prep) has developed a high resolution correlation of the submarine fans and their internal growth phases using a combination of core sedimentological logs and wireline logs from the boreholes, supported by more than 200 sedimentological logs of nearby outcrops plus continuous helicopter-based oblique aerial photography of the outcrops. The resultant physical correlation (Figs. 5–7) is considered to be accurate and thus forms a known template against which to test chemostratigraphic techniques.

For a better understanding of provenance and geochemical trends within the fan system 304 mudstone samples from cores ns1–4, covering Fan 3 to Fan 5; were chosen for the determination of major and trace elements. One centimetre slices of the core were cut approximately every metre from the fine-grained intervals between the sand-rich fans. Within the fans one centimetre slices of mudstone were sampled between the major sandstone units. Samples with interbedded coarser grained material were avoided to reduce the geochemical effects of grain size variations. The mudstone samples were jaw-crushed and pulverised in a tungsten carbide ring-and-puck mill. All samples were fused with $LiBO_2$ flux in a graphite crucible at 1000 °C for 30 min and dissolved in 5% HNO_3 (Jarvis & Jarvis, 1992a).

Samples from cores ns1, ns3 and ns4 were analysed at ACME Analytical Laboratories Ltd, Canada using an ICP emission spectrograph (Jarrel Ash AtomComp Model 975) for the determination of major elements and an ICP mass spectrometer (Perkin–Elmer Elan 6000) for trace elements. Analytical quality control included adding duplicate samples to measure the precision of the method, two analytical blanks to measure background and aliquots of in-house reference material SO-17, CSB and DS4 to measure accuracy in each analytical batch of 34 samples. SO-17, CSB and DS4 were certified in-house against 38 Certified Reference Materials including CANMET; SY-4, TILL-4, LKSD-4, STSD-1 and USGS; AGV-1, G-2, GSP-2 and W-2. Reproducibility for the major elements was generally better than 3% and for trace elements better than 5%. With reference to in-house standards (Table 1) absolute accuracy is considered generally to lie within the range of reproducibility.

Samples from core ns2 were analysed in the Department of Geology and Geochemistry, Stockholm University. The element abundances (SiO_2, Al_2O_3, $Fe_2O_3^{Tot}$, MgO, CaO, Na_2O, K_2O, TiO_2, MnO, Ba, Cr, Sc, Sr, V, Y, Zr) were measured using an ICP optical emission spectrometer (Spectro, Spectroflame Modula). Calibration curves were constructed for major and trace elements using standard reference materials. Analytical precision was determined by replicate analyses of multiple digestions of rock reference material SCo-1 and was within 3% for all major elements and 5% for trace elements. Accuracy was considered to lie within the range of reproducibility. Interlaboratory comparison of core samples and reference material SCo-1 show equivalent results.

Table 1
Results from analyses of in-house materials for assessment of analytical data quality

Element	Mean $n = 8$	SD	Official values	Upper limit	Lower limit
Majors (%)					
SiO_2	61.70	0.23	61.17	63.00	59.39
Al_2O_3	13.80	0.10	13.72	14.13	13.32
Fe_2O_3T	5.79	0.07	5.80	5.98	5.63
MgO	2.35	0.02	2.33	2.40	2.25
CaO	4.64	0.05	4.64	4.78	4.50
Na_2O	4.12	0.06	4.09	4.21	3.97
K_2O	1.41	0.02	1.37	1.44	1.30
TiO_2	0.60	0.01	0.59	0.63	0.55
P_2O_5	0.98	0.02	0.98	1.03	0.93
MnO	0.53	0.01	0.53	0.57	0.49
Cr_2O_3	0.435	0.005	0.433	0.466	0.420
Traces ($\mu g\ g^{-1}$)					
Ba	408	11	398	418	378
Co	18.9	0.6	18.7	19.7	17.7
Cu	125.4	3.4	124.7	-	-
Hf	12.2	0.5	11.9	13.1	10.7
Ni	35.1	1.8	34.5	-	-
Rb	23.4	0.6	22.8	24.0	20.6
Sc	23.4	0.5	24	27	21
Sr	306	6	300	315	285
Th	11.8	0.6	11.3	12.4	10.1
U	11.5	0.6	12.4	13.6	11.2
V	133	3	128	141	115
Y	27.0	0.4	27.2	28.5	25.9
Zr	358	3	348	365	330
La	11.0	0.4	10.5	12.0	9.0
Ce	23.5	0.6	23.0	24.2	21.8
Pr	2.92	0.08	2.88	3.02	2.74
Nd	13.0	0.6	13.7	15.1	12.3
Sm	3.3	0.1	3.1	3.4	2.8
Eu	1.03	0.05	0.99	1.08	0.90
Gd	3.75	0.09	3.91	4.30	3.50
Tb	0.68	0.09	0.65	0.72	0.58
Dy	4.18	0.04	4.16	4.37	3.95
Ho	0.93	0.03	0.89	0.98	0.80
Er	2.77	0.08	2.72	2.86	2.58
Tm	0.43	0.01	0.41	0.46	0.36
Yb	2.89	0.06	2.89	3.04	2.74
Lu	0.44	0.02	0.42	0.46	0.38

Data obtained from analyses of in-house reference materials SO-17, CSB and DS4 at ACME Analytical Laboratories Ltd which was run concurrent with the core ns1, ns3 and ns4 samples. In-house reference materials was certified against 38 Certified Reference Materials including CANMET; SY-4, TILL-4, LKSD-4, STSD-1 and USGS; AGV-1, G-2, GSP-2 and W-2.

4. Results

A complete record of the geochemical results obtained in this study from the Skoorsteenberg Formation sedimentary rocks are presented in Appendix A.

4.1. Geochemical correlation between the cores

Cluster and principal component analyses (Swan & Sandilands, 1995) show that the variance in the geochemical composition for the mudstones from different stratigraphic intervals is not statistically significant enough to discriminate them into distinct geochemical groups. Instead an empirical approach has been applied to the geochemical data. Only a few elements and element ratios show stratigraphic patterns that seem to be traceable across the basin. The ratio TiO_2/Al_2O_3, and the quantities of Zr and Sr have been plotted stratigraphically with the sedimentary logs of the four cores (Figs. 5–7). A Gaussian running mean filter (Mitchell et al., 1966) has been used to recalculate the data, giving a smoother average curve to simplify identification of potential stratigraphic trends. The interfan mudstone intervals between Fan 5A and 4 (IF5A-4) and between Fan 4 and 3 (IF 4-3) are both characterised by negative anomalies for TiO_2/Al_2O_3 and Zr and generally increasing ratios towards the base of overlying sand rich fans. A distinct positive Sr peak can also be seen in the IF5A-4. Intrafan mudstones of Fan 4 (F4) have medium to high ratios of TiO_2/Al_2O_3 and Zr while the Sr ratios increase upward throughout this whole interval. In ns1, ns3 and ns4 Fan 4 contains mudstones that have relatively high (>250 μg g^{-1}) Zr content.

Taylor and McLennan (1985) showed that Zr occurs mostly in the heavy mineral assemblage and thus fractionates together with quartz and feldspar into the coarse fraction. The elevated Zr quantities in Fan 4 might best be explained by a higher sand and silt ratio in these samples. However a plot of Zr against SiO_2 (which can be a good proxy for coarser grained material) from ns1 mudstones and sandstone samples from outcrop (Fig. 8 and Appendix A), show a group of samples that diverge from the general trend and are considerably enriched in Zr relative to SiO_2. These anomalous samples have unusually high Zr that cannot be related to sand enrichment in the sediment.

Sr quantities generally decrease from F5A through IF 5B-5A to Fan 5B, otherwise these intervals do not show any diagnostic geochemical trends that can be traced across the basin.

4.2. PAAS normalised data

The distribution of major and trace elements in the Skoorsteenberg Formation mudstones has been examined in a multi-element diagram. The plot in Fig. 9 compares average ratios of major and trace elements for each stratigraphic interval against a normalised shale standard, the post-Archean average shale (PAAS; Taylor & McLennan, 1985). The main feature to note is the degree of conformity of the values with those of the PAAS. Most element values are evenly spread out around the PAAS values although certain components (Na_2O, Rb Y, Th, U) show a slight enrichment and others (CaO, Sr, Cr, V, Ni) a slight depletion, for nearly all inter- and intra-fan mudstones.

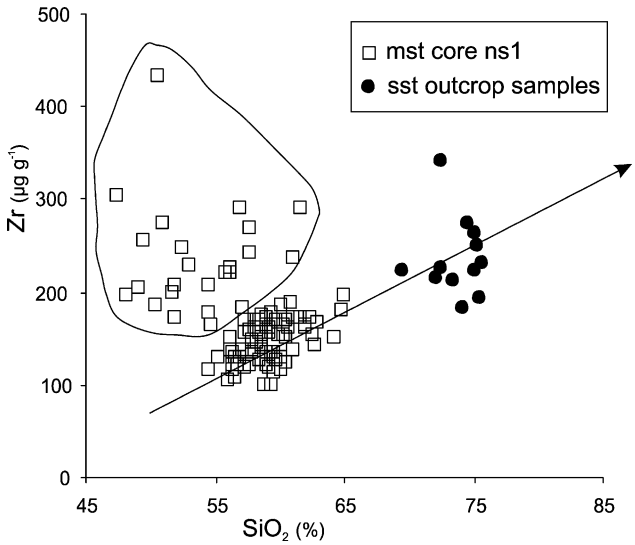

Fig. 8. Bivariate plot of SiO_2 and Zr for mudstones from core ns1 and outcrop samples of sandstones from Fan 1 to Fan 5B (Appendix and Fig. 6). The majority of the mudstones show a positive correlation with SiO_2 and Zr and follow a regression line where the sandstone samples represent the coarse grained end member. A group of mudstones (encircled), mainly derived from Fan 4, diverge from this trend and are considerable enriched in Zr relative to their SiO_2 ratios.

4.3. REE data

Rare-earth element (REE) data are conventionally interpreted in terms of a comparison to internationally accepted standards. The REE data have thus been normalised to chondritic meteorites (Taylor & McLennan, 1985). The results of REE analyses of core ns1, ns3 and ns4 are shown, together with PAAS (Taylor & McLennan, 1985) and two reference samples; granite G1 and dolerite W1, as chondrite-normalised patterns in Fig. 10. The chondrite-normalised REE spectra for the Skoorsteenberg Formation mudstones are characterised by significant enrichment of light REEs (where the LREE include La, Ce, Nd, Pr, Nd, Sm), relative to heavy REEs (where the HREE include Gd, Tb, Dy, Ho, Er, Tm, Yb, Lu) and the presence of a pronounced negative Eu/Eu* anomaly (0.56–0.63) comparable to typical post Archean average shales ($Eu/Eu^* = 0.65 \pm 0.5$). The Eu/Eu^* anomaly was calculated as follows:

$$Eu/Eu^* = EuN/[(Sm_N)(Gd_N)]^{1/2}$$

The subscript N denotes chondrite-normalised values and Eu^* represents the Eu value expected for a smooth chondrite-normalised REE pattern (McLennan, Taylor, McCulloch, & Maynard, 1990).

4.4. Stratigraphy vs geochemistry

Linear regression models have been produced to display the abundance of elements and element ratios relative to stratigraphic intervals in order to show time-related trends in

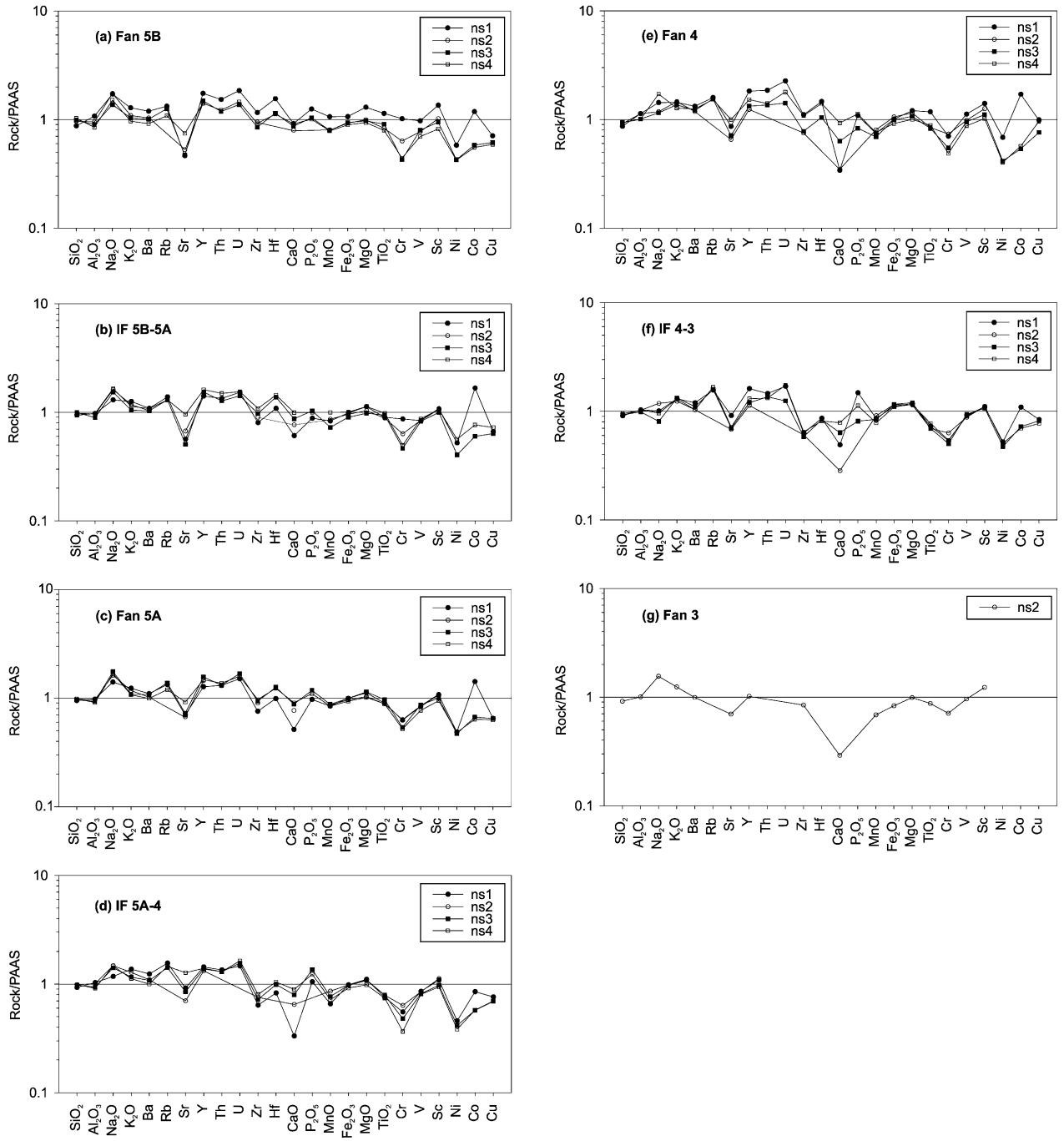

Fig. 9. Average PAAS normalised element ratios for mudstones of F5B (a), IF5B-5A (b), F5A (c), IF5A-4 (d), F4 (e), IF4-3 (f), F3 (g). Note the relative enrichment in Na_2O, Rb Y, Th, U and slight depletion in CaO, Sr, Cr, V, and Ni for nearly all intervals.

the mudstones of the Skoorsteenberg Formation (Fig. 11). In the figures, circles represent group medians. Vertical bars represent errors on the estimated averages at a 95% confidence level. The statistical function *p* that is shown on each graph reflects the probability that the slope of a regression line through the data is zero (i.e. there is a change in the parameter as a function of stratigraphic position). The smaller the *p* number, the higher the probability that the line slope is non-zero. Data distributions with p values of 0.050 or less show time-related trends that are significant at, or above, the 95% level. Data distributions that have p values greater than 0.050 do not show statistically significant trends (Cox et al., 1995; Swan & Sandilands, 1995).

5. Discussion

5.1. General geochemical composition

Normalised multi-element data (Fig. 9) and chondrite normalised REE patterns (Fig. 10) from the Skoorsteenberg

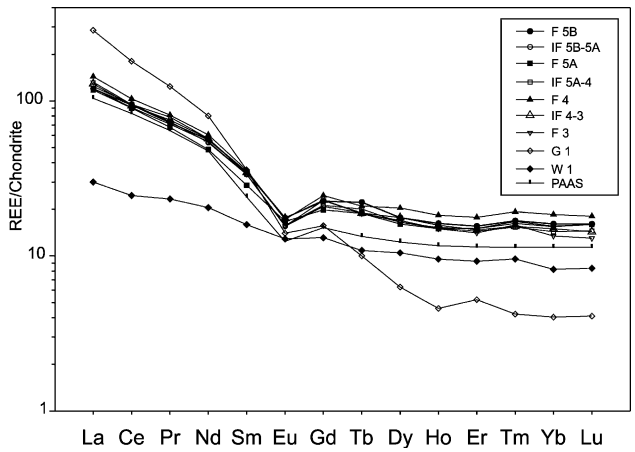

Fig. 10. Comparison of average chondrite-normalised REE pattern of the interfan and intrafan mudstone intervals of Skoorsteenberg Formation and a granite (G1), dolorite (W1) and PAAS. Chondrite normalizing factors and PAAS are from Taylor and McLennan (1985), G1 and W1 from Mason and Moore (1982).

Formation mudstones generally show a good conformity with the PAAS values. The PAAS standard is considered to reflect the upper continental crust (McLennan, 1989) and the overall geochemical data set from the mudstones points towards a similar source terrain. Subtle deviations from the PAAS values, however, have been identified in the Skoorsteenberg Formation and the implications of these are discussed below.

Enrichment of Na_2O may be due to the presence of abundant plagioclase feldspar (albite) in the coarser grained fraction of the mudstones. Petrographic and electron microprobe studies of sandstones from Fan 3 revealed that the sandstones are arkoses with more than 25% feldspar and that quartz and albite are the dominant minerals (Den Boer, 2002). It should also be noted that the highest Na_2O ratios (>1.70) are from the intrafan mudstones, suggesting a higher silt and sand component than in the interfan mudstones, in agreement with previous sedimentological studies (Johnson et al., 2001).

In contrast to CaO, Na_2O and Sr, which are relatively mobile and can be lost from a mudstone, Rb tends to be incorporated into clay minerals by adsorbtion and cation exchange during chemical weathering of fresh continental rock (Nesbitt, Markovics, & Price, 1980). A strong negative correlation between Na_2O and Rb ($r = -0.75$) indicates that clay minerals in the clay mineral-rich fraction host the Rb. Elevated Rb and depleted CaO and Sr relative to PAAS might suggest more intense weathering conditions in the hinterland but could alternatively be explained by a more felsic, Rb-rich source rock. Incompatible elements such as Rb, Y, Th and U are preferentially fractionated into melts during crystallization (e.g. Hall, 1996 and references therein) and as a result these elements are enriched in felsic rather than mafic rocks. The relative depletion of the ferromagnesian-associated elements Cr, V, and Ni, commonly associated with mafic rocks, also support a slightly more felsic source terrain in comparison to PAAS.

The Skoorsteenberg Formation mudstones are slightly enriched in both HREE and total REE relative to PAAS. The REE are strongly incompatible elements that are concentrated in partial melts and so should be enriched in sediments derived from granitic rocks (Cox et al., 1995). The relatively higher total REE ratios, therefore, typically reflect more fractionated igneous material in the source terrain relative to the upper continental crust. The slight enrichment of HREE could be explained by high concentrations of heavy minerals such as zircon and garnet which are fractionated in HREE relative to LREE. However Zr/Yb ratios are typically greater than 1000 in zircon (Taylor & McLennan, 1985) and 100–200 ppm higher Zr concentrations relative to PAAS (210 ppm) would be required to account for the recorded Yb enrichment (Fig. 10 and Appendix A). Fig. 9 show that the PAAS normalised Zr concentrations are evenly distributed around 1. The presence of garnet (e.g. pyrope and almandine), which has much lower Zr/Yb ratios than zircon, has been reported from the sandstones of the Skoorsteenberg Formation (Scott, 1997). A relatively small enrichment in the mudstones of this heavy mineral may account for the high HREE concentrations.

5.2. Inter- and intra-fan mudstone sources within and between fans in turbidite systems

An important issue in deep-water sedimentary systems is the supply of the sedimentary material. In terms of the finest fractions, this distils down to the question of whether mudstone found as thin layers within turbidite fans has the same source as much thicker mudstone packages that occur between sand-rich fans. Does the mud that gets deposited during short-duration sea level cycles have the same origin as that deposited during longer-term periods of sea level rise and storage of sand on the coeval shelf?

Despite distinct anomalies, there are quite pronounced geochemical temporal trends in the entire successions (Fig. 11). The interfan mudstones and the intrafan mudstones seem to form part of the same evolutionary pattern since the changes occur for all the mudstones. For example, the $K_2O/(K_2O + CaO)$ patterns typically decrease up the stratigraphic section in all wells for both mudstone types. The homogeneity of the patterns through all mudstones strongly suggests that the sediments in both interfan and intrafan mudstones have one common origin. The patterns lead us to conclude that there is only one discernible source for both the intrafan and interfan mudstones. There is thus no need to examine the sedimentary system for discrete sources of mud.

This interpretation of core geochemistry differs from the interpretation of the outcrop geochemical study (Andersson & Worden, in press) where there were differences in SiO_2, TiO_2/Al_2O_3, Zr and Y between the interfan and intrafan

mudstones. The uniformity in mudstone character reported in this core study may result from the exclusion of Fan 1 and Fan 2 from this study (Fans 1 and 2 were not cored), the effects of weathering in outcrop (possibly preferentially altering one type of mudstone) and/or the outcrop study involving fewer samples (with less certainty of the results). It is difficult to assess the significance of the different conclusions from the two types of geological material although we have more confidence in the geochemical data from the (absolutely unweathered) core reported in the present study.

5.3. Stratigraphic variation and provenance evolution

The (CIA = $[Al_2O_3/(Al_2O_3 + CaO^* + Na_2O + K_2O)] \times 100$) has been interpreted as an indicator of major element changes due to weathering and the conversion of feldspars, volcanic glass and other labile components to clay minerals (Nesbitt & Young, 1982). The CIA, therefore, could potentially be a useful index to characterise mudstones in terms of the degree of weathering of the sediment source and in terms of variable source terrains for the Skoorsteenberg Formation. Worldwide average shale CIA values range between about 70 and 75; fresh granites give values of around 50 (Visser & Young, 1990) while extreme weathering could produce values approaching 100. Mudstones of the Skoorsteenberg Formation all have CIA values between 58.8 and 72.6 indicative of a slightly to moderately weathered source terrain. There is a significant decrease in CIA values up the stratigraphic succession ($p < 0.001$ to $p = 0.004$). In order to eliminate the possibility that aluminium is the pre-eminent controlling factor on the CIA trend, Al_2O_3 has been plotted in the same manner. The results show that Al_2O_3 remains approximately constant throughout the stratigraphic intervals and has relatively higher p values ($<0.001-0.025$) indicating that variations of CaO, Na_2O and K_2O must dominate the observed CIA trend. It thus seems that the source terrain underwent progressively less intense weathering over the time period of the deposition of the Skoorsteenberg Formation. Less intense weathering might have been the result of either a cooler or less humid climate, or some combination of these two changes. On the other hand a tectonically active hinterland with progressive uplift of younger igneous rocks and high erosion rates might also produce successively more unweathered material and hence decreasing CIA values.

Trace elements are usually considered to be a more useful indication of the tectonic setting than the major elements, discussed above, due to their very short residence times in freshwater or seawater and their characteristic behavior during fractional crystallization, weathering and recycling (Taylor & McLennan, 1985). Some of the element abundances and element ratios commonly used in the literature in provenance studies (Bhatia & Crook, 1986; McLennan et al., 1990; Floyd, Shail, Leveridge, and Franke, 1991) here reveal no discernable variations with stratigraphic position in the Skoorsteenberg Formation (Appendix A). REE have historically been applied to many rock types to help decipher the origin and provenance evolution of rocks (Bhatia, 1985; Davies & Pickering, 1999; McLennan et al., 1990; Vital et al., 1999). Given the relative uniformity of the chondrite normalised rare earth element pattern it is possible to conclude that the landmass that contributed sediment to the Skoorsteenberg Formation was relatively constant and that one dominant terrain supplied the sediment.

The La/(La + Lu) ratio succinctly mirrors the fractionation of the light REE relative to the heavy ones. In basaltic and andesitic melts the REEs are incompatible in minerals such as olivine, orthopyroxene and clinopyroxene and are only slightly fractionated. Most upper-crustal granitic rocks are thought to have been derived through partial melting of the crust (Wyllie, 1977) and should therefore be fractionated in the same way. Fig. 10 demonstrates the considerably more fractionated REE pattern for a reference granite G1 relative to a dolerite W1. A statistically significant ($p = 0.001$) decrease in La/(La + Lu) ratios up the stratigraphy, meaning less fractionation (where decreasing fractionation implies an increasing ratio of mafic to grantic source material), can be seen from core ns1 and ns3 (Fig. 11). La/(La + Lu) data from core ns4 show little stratigraphic variation ($p = 0.530$) and seemingly do not support the trend seen from the other two cores.

Th and Y are elements that are enriched in felsic rather than mafic rocks. However, geochemical analyses of reference rocks (Govindaraju, 1989) show that the relative enrichment is generally much greater for Th than for Y in granites in comparison to basalts. Decreasing Th/(Th + Y) ratios ($p < 0.001$ to $p = 0.064$) up the stratigraphy can be seen in core ns1, ns3 and ns4. This trend suggests an increase of a mafic component in the sediment supply with time. Hf occurs in many different minerals but replacement for Zr in zircon is by far the most mineralogically common site for this element. Abundances of Zr and Hf generally

Fig. 11. Abundance and ratios of major and trace elements as a function of stratigraphic intervals. Dots represent individual data points. Circles represent group medians. Vertical bars represent errors on the estimated averages at a confidence level of 95%. The p statistical function shown on each graph reflects the probability that the slope of a regression line through the data is zero (i.e. no regular variation with stratigraphy). The smaller the number, the higher the probability that the line slope is non-zero: i.e., data distributions with p values of 0.0500 or less show time-related trends that is significant at or above the 95% level. Data distributions that have p values greater than 0.0500 do not show significant trends with stratigraphy. The r value (correlation coefficient) is a measure of the goodness-of-fit for the regression line. CIA values (CIA) were determined using mole proportions, as follows; CIA = $[Al_2O_3/(Al_2O_3 + CaO^* + Na_2O + K_2O)] \times 100$ where CaO^* is defined as CaO in the silicate fraction (Nesbitt & Young, 1982). In this study there was no objective way to distinguish carbonate CaO from silicate CaO, so total CaO is plotted here. This is justified on the basis that none of the samples appeared calcareous and all samples except five contained less than 1% CaO (Appendix A).

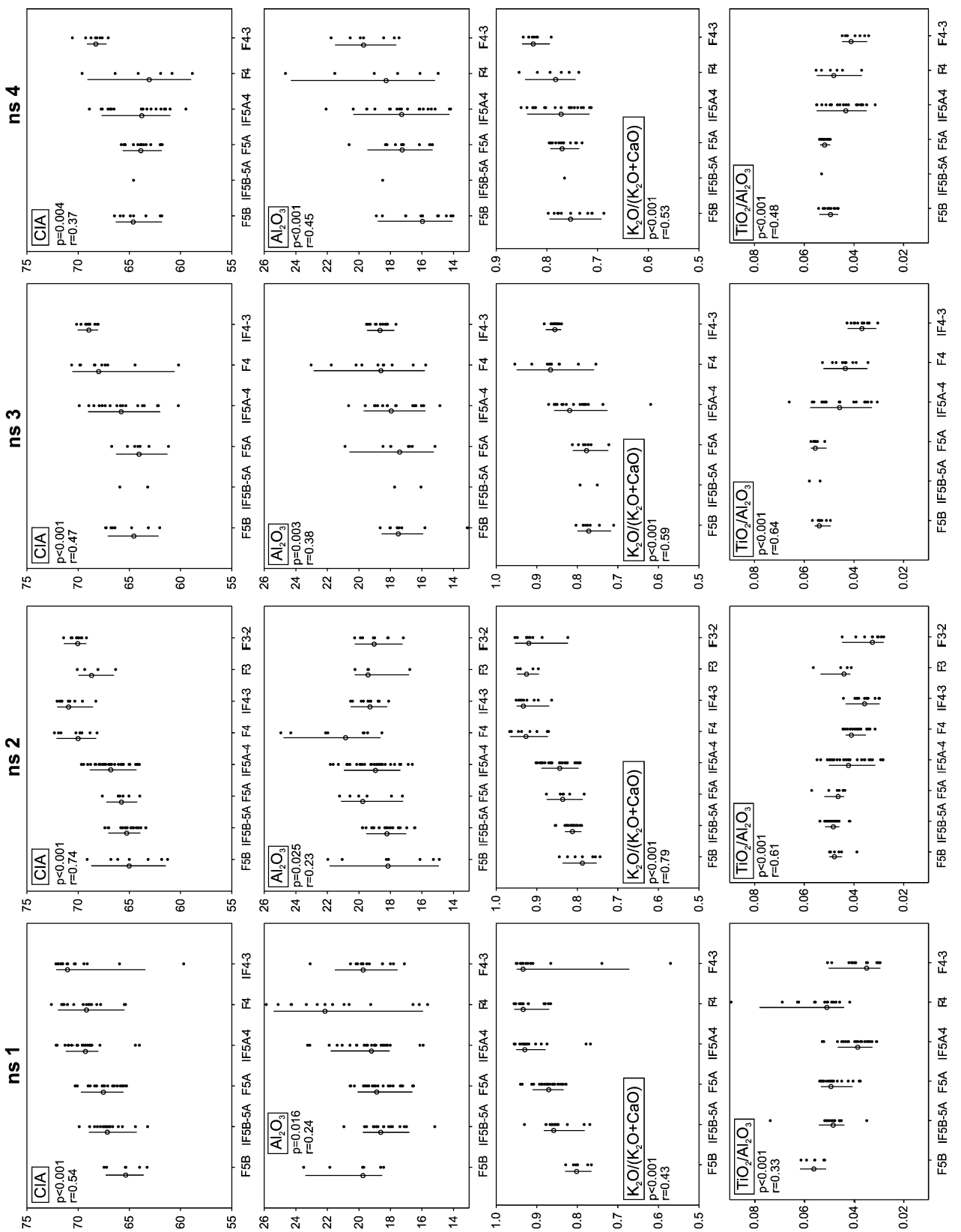
ns 1
ns 2
ns 3
ns 4
CIA
p<0.001
r=0.54
p<0.001
r=0.74
p<0.001
r=0.47
p=0.004
r=0.37
Al2O3
p=0.016
r=0.24
p=0.025
r=0.23
p=0.003
r=0.38
p<0.001
r=0.45
K2O/(K2O+CaO)
p<0.001
r=0.43
p<0.001
r=0.79
p<0.001
r=0.59
p<0.001
r=0.53
TiO2/Al2O3
p<0.001
r=0.33
p<0.001
r=0.61
p<0.001
r=0.64
p<0.001
r=0.48
F5B IF5B-5A F5A IF5A4 F4 IF4-3 F3 F3-2 F4-3

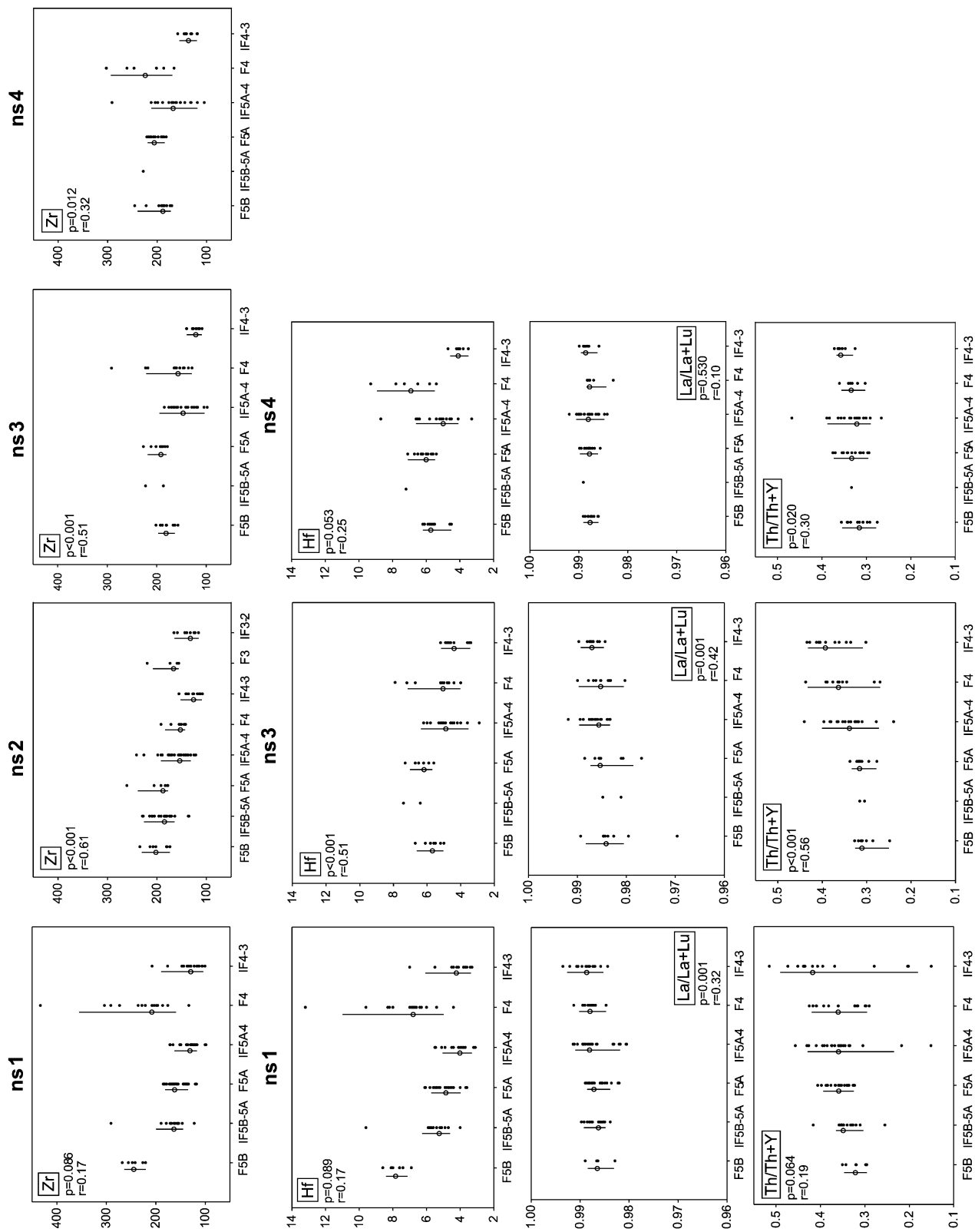

Fig. 11 (*continued*)

increase up the stratigraphy with statistical significance in nearly all of the cores (Figs. 6 and 11). Increasing Zr and Hf abundance with time (Fig. 11) suggests, contrary to the other element trends, that there seems to have been an increase in supply of a felsic or recycled source (Bhatia & Crook, 1986) with time.

TiO_2 and Al_2O_3 are refractory oxides that are highly resistant to weathering in all but the most extreme environments, for example in long-lived weathering profiles in hot and humid conditions (Hill, Worden, & Meighan, 2000a). In mudstones, Al is broadly indicative of the overall clay content, while in sandy sediments, TiO_2 can be abundant in heavy minerals such as rutile, ilmenite or anatase. However, significantly for mudstones, TiO_2, together with Cr and Sc are elements that can be characteristic of primary, pre-weathering, ferromagnesian minerals such as biotite, amphibole, pyroxene and olivine (Nesbitt, 1979; Taylor & McLennan, 1985). These high-temperature minerals alter readily to clay minerals so that variation in the TiO_2 content of a clay-rich rock may reflect variations in the initial rock material that weathered to clay. It is unlikely that TiO_2 represents the presence of heavy minerals since these are concentrated in the coarser grained fractions and are thus relatively unlikely to be present in mudstones. Individually, mudstone TiO_2 and Al_2O_3 contents might vary due to dilution by quartz, calcite or other non-clay minerals, so that it is best to use a ratio of these two resistant oxides as an indictor of provenance. The mudstone TiO_2/Al_2O_3 ratios show a significant ($p < 0.001$) increase up the stratigraphic succession in all wells (Figs. 5 and 11). The geochemical data reveal subtle stratigraphic changes. These are best viewed by examining the entire mudstone database on a well-by-well basis and by grouping the data into discrete clusters for each fan and for each interfan body (Fig. 11). The increasing ratio of TiO_2/Al_2O_3 as well as the increasing quantities of Zr and Hf can be seen in the data (Figs. 5, 6, and 11). In addition to TiO_2, Zr and Hf are considered to be highly resistant elements although mobility during extreme weathering has been reported (Hill, Worden, & Meighan, 2000b). In all of the mudstones, stratigraphic evolution patterns in the TiO_2/Al_2O_3 ratios are reasonably well defined as are increasing Zr and Hf quantities. There are three possible ways to explain the stratigraphic variation in the mudstones:

1. One single source terrain underwent increasingly extreme degrees of weathering from mild to extreme (required to mobilise Al relative to Ti);
2. One sediment source terrain underwent progressive denudation and incision into different bedrock lithologies. The more deeply buried and later exposed bedrock was presumably more mafic than the first exposed rocks.
3. Two completely isolated source terrains supplied sediment in steadily changing proportions through time.

Mudstones vastly dominate the sedimentary fill in the majority of the global basins. Blatt (1970) estimated that close to 65% of the sedimentary record is made up of mudstones, 25% of sandstones and 10% of carbonate rocks. Element concentrations of the PAAS may therefore be used as a proxy for sedimentary and metasedimentary source rocks in comparison to felsic and mafic igneous source rocks. TiO_2/Al_2O_3 ratios increase from approximately 0.03 below Fan 4 to 0.06 at the top of Fan 5B in core ns1 (Fig. 11 and Appendix A). Corresponding average ratios of rock reference granites and gabbros (Govindaraju, 1989) are 0.02 and 0.17, respectively, while the PAAS have an intermediate ratio of 0.05. The easiest way to explain the increasing TiO_2/Al_2O_3 ratios up-section would be a progressive increase of a mafic igneous component to the sedimentary system. The decreasing CIA counters option 1 above. The CIA values are everywhere indicative of a mild weathering regime. Indeed the weathering seemingly became less intense with time.

Although potassium is thought to be highly soluble in water it tends to be conserved in mudstones because of the chemical stability of illite (Norrish & Pickering, 1983). Illite is relatively resistant to weathering and is potentially stable in soils except under extreme weathering conditions (Norrish & Pickering, 1983). In poorly weathered material K_2O may represent the amount of felsic material in the rock while CaO may represent the mafic component. From the stratigraphic data, the ratio of $K_2O/(K_2O + CaO)$ shows a significant ($p < 0.001$) decrease with time. Alternatively progressively more mafic sediment could have been supplied since the former ratio is a proxy for a K-feldspar-plagioclase ratio. La/(La + Lu) and Th/(Th + Y) ratios also show decreasing signals with time supporting option 2 above. These trends are not as statistically rigorous as for the other parameters. The relative uniformity of the chondrite normalised rare earth element pattern (Fig. 10) suggest that option 3, above, is not generally viable.

The increasing Zr and Hf values up-section are seemingly in contradiction to option 2 above (the bedrocks undergoing weathering in the hinterland became more mafic with time). Zr and Hf are routinely enriched in granitic (felsic) rocks. The Zr content in the Skoorsteenberg Formation increases from approximately 120 ppm below Fan 4 to 280 ppm at the top of Fan 5B in core ns1 (Fig. 11 and Appendix A). Average Zr concentrations of rock reference granites and gabbros (Govindaraju, 1989) are 245 and 120 ppm, respectively, and 200 ppm for the PAAS. A progressive denudation of a Zr rich granitic source rock could best explain the increase in Zr content with time. The anomalous increase of both mafic and felsic signals could be explained by the bedrock (sediment source terrain) becoming enriched in granitic rocks as well mafic rock, relative to the initial sediment-supplying rocks. Signals that decrease up-section such as $K_2O/(CaO + K_2O)$, La/(La + Lu) and Th/(Th + Y) are direct indicators of the mafic/felsic contribution to the sediment supply so that while the granitic supply might have increased in absolute terms, the mafic supply must have increased even more.

The overall picture that emerges from the data is somewhat paradoxical, the mudstones of the Skoorsteenberg Formation had one pre-eminent source and display major and trace element patterns that indicates increasing input from both mafic and felsic sources in the hinterland with time.

5.4. Implications for the evolution of the sedimentary systems: source, climate, dispersal, hinterland evolution

The previous discussion led to the general conclusion that there was one evolving source terrain that was being progressively unroofed into rocks of increasingly igneous type. The source terrain supplied sediments that were overall slightly more felsic in comparison to PAAS. However, the more deeply buried and progressively denuded rocks must have been predominantly mafic to have led to the changes characteristic of the succession. It is worth reiterating that the CIA decreases up the stratigraphy in all wells. One possible explanation for this is that the weathering regime became less intense with time. Such a conclusion is a vital clue to the reconstruction of the conditions that gave rise to the sedimentary succession. However the CIA data no more than suggest that the climate changed (to less humid and/or cooler) during the generation of the sediments of the Skoorsteenberg Formation. Proof must come from other sources.

In many of the changing geochemical data patterns, there is a common anomaly of varying magnitude. Fan 4 displays unusual data for many parameters in many wells. The clearest anomalies lie in the Zr data in Fig. 6 and in Zr, Hf and TiO_2/Al_2O_3 data in Fig. 11. Zr, Hf and TiO_2 are elements often associated with heavy mineral assemblages in sedimentary rocks and thus fractionate towards the coarse grained fraction. If selective size-sorting were the only process responsible for the elevated Zr ratios it might be anticipated that the samples would plot on a slope between fine and coarse grained samples as shown in Fig. 8. However a divergent group of samples (mainly from Fan 4) that are relatively low in SiO_2 and high in Zr instead suggest enrichment of Zr, Hf and TiO_2 due to a 'true' change in composition of the source rock rather than dilution by silt or sand. Palaeocurrent data suggest that Fan 4 was derived from the west to southwest rather than from the south (Wickens, 1994; Fig. 4). The anomalies may thus be accounted for by suggesting that at least some of the sediment in Fan 4 may have had a slightly different source terrain to the bulk of the sediment in the fans and interfan mudstones, or a different shelf and slope transport regime. The geochemical data thus support the sedimentological data since the intrafan mudstones in Fan 4 have a slightly different provenance than the rest of the mudstones. Although the overall geochemical character, and thus source type, of these mudstones is similar to the others there are subtle differences that show up through many geochemical parameters.

5.5. Chemostratigraphy and correlation of turbidite systems

The correlation of geological formations is a perpetual issue when there is an incomplete picture of the rocks (e.g. in the subsurface over great distances). For turbidites the question distils down to the way in which discrete sand-prone intervals in various wells should be correlated. We aimed to see whether geochemical data could provide a viable mechanism for deciding on, or supporting, detailed correlation schemes. The logs presented in Figs. 5–7 show some of the benefits and problems of geochemical correlation. The continuous log shows a relatively noisy pattern that could not easily be used for ab initio correlation in the absence of other data types. The smoothed logs, produced by running a Gaussian filter, helps somewhat to remove the noise but it also makes the trends relatively bland thus removing detailed correlation possibilities. If the geochemical data were produced for these four wells with no supporting core or wireline data, correlation would not be possible with any degree of confidence. The geochemical data have proved to be useful indicators of the nature and evolution of the sediment hinterland but they cannot easily yield credible independent high resolution correlations of mudstone units.

5.6. Lateral differences within mudstone units

Most of the fan and interfan mudstones display the same general stratigraphic variations (Figs. 5, 6, 7 and 11). This observation strongly suggests that there are limited proximal to distal and axial to marginal changes along the general sediment dispersal pattern. The uniformity of the geochemical signals shows that they are robust to the inevitable depositional variations that occur in all widespread sedimentary depositional systems. It shows that mudstone geochemical signals are insensitive to minor changes in sediment flux or the exact locus of sedimentation.

6. Conclusions

1. Geochemical data from one sedimentary rock type (mudstones) have helped to reveal details about the evolution of the long-vanished hinterland, palaeoclimate and sediment dispersal patterns.
2. The geochemical data from major and trace elements, including rare earth elements, have helped to demonstrate that the mudstones that are interbedded with turbidite fan sandstones probably have the same origin as the mudstones in thick interfan successions.
3. The geochemical data have also helped to reveal subtle changes in mudstone provenance up the stratigraphic succession. The changes include increasing TiO_2/Al_2O_3, Zr and Hf and decreasing Sr, $K_2O/(CaO + K_2O)$, CIA, $Th/(Th + Y)$ and $La/(La + Lu)$ although some

Appendix A

Core	Stratigr level	SiO2 %	Al2O3 %	Fe2O3 %	MgO %	CaO %	Na2O %	K2O %	TiO2 %	P2O5 %	MnO %	LOI %	SUM %	Cr ppm	Ba ppm	Co ppm	Cu ppm	Hf ppm	Ni ppm	Rb ppm	Sc ppm	Sr ppm	Th ppm	U ppm	V ppm	Y ppm	Zr ppm	La ppm	Ce ppm	Pr ppm	Nd ppm	Sm ppm	Eu ppm	Gd ppm	Tb ppm	Dy ppm	Ho ppm	Er ppm	Tm ppm	Yb ppm	Lu ppm
ns1	5.04	55.79	19.69	6.97	2.81	1.14	2.11	4.54	1.02	0.21	0.11	5.3	99.79	41.1	723	30.4	31.7	6.9	33.3	196.7	20	90	19.6	3.9	139	41.6	221	35.6	80.6	8.88	35.5	8.1	1.6	6.98	1.15	6.75	1.37	4.17	0.66	3.84	0.62
ns1	6.40	52.57	21.84	6.98	3.09	1.23	1.68	5.23	1.29	0.16	0.12	5.5	99.80	58.2	819	19.8	38.3	8.1	33.3	233.2	26	74	24.2	5.9	155	46.4	247	53.5	105.6	11.76	45.1	9.6	1.9	8.11	1.28	7.66	1.53	4.62	0.68	4.68	0.74
ns1	6.58	49.57	23.50	6.99	3.14	1.25	1.54	6.04	1.31	0.22	0.11	6.0	99.80	75.3	903	21.7	42.9	7.6	31.3	275.6	27	75	26.9	8.2	173	49.8	255	57.5	112.5	12.50	46.9	9.7	1.9	8.47	1.40	8.16	1.66	4.92	0.75	4.82	0.78
ns1	8.91	57.65	18.62	6.80	2.62	1.21	2.65	3.94	1.04	0.21	0.12	4.8	99.77	78.7	712	39.6	31.2	8.0	30.7	179.6	19	116	19.9	4.9	136	46.8	242	60.9	120.2	13.43	50.3	10.4	2.1	7.91	1.34	7.96	1.62	4.72	0.72	4.61	0.68
ns1	12.56	56.13	19.76	6.85	2.79	1.13	2.07	4.63	1.03	0.21	0.12	5.0	99.82	27.4	799	23.4	33.8	7.4	30.7	199.9	18	98	19.7	5.2	129	46.9	226	50.0	98.2	11.17	43.4	9.3	1.8	8.29	1.29	7.94	1.54	4.57	0.72	4.66	0.69
ns1	13.91	57.79	18.43	6.89	2.68	1.19	2.31	4.08	1.13	0.19	0.12	5.0	99.91	54.7	693	28.1	34.4	8.6	31.5	187.2	20	104	23.8	6.2	144	50.7	268	54.5	110.1	12.40	47.8	10.2	1.9	8.51	1.34	8.49	1.71	4.88	0.71	4.74	0.74
ns1	15.70	56.99	18.87	6.40	2.68	1.39	2.10	4.63	1.39	0.25	0.10	4.9	99.80	41.1	742	32.8	58.7	9.6	35.9	224.4	25	108	31.2	10.2	149	57.6	291	65.8	132.1	14.72	55.3	11.6	2.1	9.33	1.64	9.35	1.98	5.64	0.87	5.64	0.96
ns1	16.95	60.46	18.11	6.19	2.43	0.70	1.70	4.46	0.88	0.13	0.09	4.6	99.85	47.9	726	23.8	31.4	5.7	28.5	208.6	15	88	18.0	4.6	114	32.5	168	41.0	81.2	8.87	34.8	6.6	1.1	5.52	0.89	5.35	1.08	3.14	0.50	3.17	0.52
ns1	18.06	57.38	19.64	6.76	2.61	0.73	1.28	5.22	0.90	0.13	0.09	5.1	99.94	47.9	714	20.8	30.8	4.9	25.6	254.4	18	85	20.7	4.1	139	38.0	155	45.4	92.6	9.78	37.1	7.3	1.2	6.27	1.05	6.74	1.29	3.93	0.59	4.09	0.65
ns1	19.17	58.09	19.07	6.63	2.53	0.80	1.45	4.71	0.93	0.14	0.09	5.3	99.84	41.1	700	16.0	33.1	5.7	27.1	221.2	19	89	18.9	4.9	133	36.7	163	39.3	80.5	8.84	33.3	7.0	1.2	6.22	1.01	6.01	1.18	3.74	0.57	3.45	0.60
ns1	20.01	59.08	19.02	6.34	2.40	0.67	1.36	4.76	0.93	0.14	0.08	5.0	99.88	75.3	689	77.8	28.8	5.2	27.9	228.8	17	94	19.4	4.7	126	35.5	163	35.3	71.1	8.03	31.2	6.7	1.2	5.64	0.98	5.77	1.22	3.32	0.54	3.49	0.58
ns1	20.91	58.24	19.03	6.62	2.56	0.76	1.39	4.96	0.86	0.11	0.09	5.1	99.82	44.5	712	33.1	28.5	4.7	32.4	234.0	18	96	19.2	3.7	126	38.6	147	42.1	83.3	9.46	36.9	7.7	1.3	6.38	1.07	6.33	1.37	3.71	0.59	3.99	0.60
ns1	21.68	64.88	15.19	6.08	2.05	0.92	1.91	3.32	0.77	0.16	0.09	4.1	99.56	54.7	659	225.9	35.1	5.9	27.4	152.5	13	109	15.3	3.5	89	44.7	179	40.1	83.3	9.77	39.0	8.8	1.6	8.13	1.26	7.46	1.50	4.05	0.69	4.00	0.58
ns1	22.78	59.86	17.98	6.46	2.49	0.78	1.52	4.62	0.82	0.12	0.09	5.1	99.93	30.8	706	25.2	32.1	4.7	28.7	216.6	16	112	18.1	3.9	116	37.3	154	48.3	95.3	10.47	39.5	7.5	1.4	5.56	1.05	6.08	1.22	3.53	0.56	3.57	0.56
ns1	23.59	56.44	20.95	6.14	2.52	0.45	1.05	6.00	0.73	0.08	0.08	5.3	99.84	47.9	759	18.2	29.4	4.0	27.9	299.9	18	95	18.2	4.1	147	25.5	122	31.1	61.7	6.67	24.9	5.1	0.8	4.04	0.66	3.74	0.84	2.60	0.43	2.75	0.47
ns1	24.59	58.03	19.08	6.55	2.66	0.79	1.40	5.02	0.86	0.13	0.10	5.1	99.82	58.2	726	22.5	35.3	5.1	30.2	259.3	17	128	21.0	4.2	142	39.2	169	57.9	112.6	12.35	44.8	9.0	1.5	6.45	1.09	6.40	1.28	3.90	0.60	3.93	0.60
ns1	25.81	60.90	17.39	6.34	2.44	0.90	1.76	4.22	0.90	0.16	0.10	4.7	99.90	44.5	684	31.0	37.6	5.8	27.5	203.4	16	128	19.2	4.4	122	40.8	189	56.7	112.8	12.48	45.2	8.8	1.5	6.83	1.16	6.81	1.44	4.11	0.65	4.15	0.62
ns1	26.68	59.12	18.44	6.57	2.61	0.83	1.60	4.72	0.92	0.14	0.10	4.8	99.94	47.9	699	17.8	29.4	5.2	32.5	206.5	17	111	19.7	4.7	122	36.0	157	46.0	92.1	10.19	38.2	7.7	1.2	6.10	1.04	5.89	1.20	3.54	0.53	3.58	0.56
ns1	27.42	58.94	18.79	6.56	2.49	0.78	1.53	4.81	0.90	0.14	0.09	4.8	99.92	44.5	727	20.3	33.0	5.6	27.6	242.2	17	143	21.1	4.7	142	39.4	171	47.3	97.0	10.84	41.5	7.9	1.4	6.50	1.08	6.51	1.31	3.96	0.61	4.08	0.66
ns1	28.22	57.34	19.51	6.72	2.63	0.81	1.52	5.03	0.93	0.14	0.10	5.1	99.93	41.1	733	29.0	31.8	5.6	28.1	253.5	19	144	21.5	5.2	144	40.3	169	45.1	90.9	10.39	37.9	7.8	1.5	6.84	1.09	6.56	1.33	3.77	0.64	4.16	0.65
ns1	29.65	59.73	18.41	6.29	2.51	0.78	1.62	4.58	0.94	0.15	0.09	4.6	99.80	58.2	679	41.7	33.5	5.4	30.8	211.6	18	124	20.1	5.1	132	36.0	170	49.9	99.7	10.71	39.7	7.7	1.4	5.91	0.94	5.87	1.18	3.40	0.58	3.60	0.60
ns1	30.41	61.99	17.12	6.21	2.34	0.76	1.74	4.21	0.84	0.16	0.10	4.3	99.87	34.2	708	20.5	32.9	5.1	28.6	194.0	15	125	16.0	4.4	109	35.5	161	48.5	96.9	10.58	38.9	7.5	1.3	5.86	0.97	5.66	1.20	3.31	0.56	3.33	0.53
ns1	31.22	62.48	16.98	6.35	2.27	0.72	1.62	4.09	0.82	0.13	0.08	4.2	99.83	37.6	662	18.5	26.6	4.7	26.2	181.9	14	126	17.1	4.4	102	34.9	154	42.2	84.3	9.30	34.9	7.1	1.3	6.11	0.91	5.80	1.16	3.20	0.51	3.50	0.53
ns1	31.91	60.29	17.87	6.42	2.33	0.71	1.57	4.49	0.82	0.13	0.09	5.1	99.93	61.6	689	17.3	30.0	4.9	25.0	202.4	16	132	18.3	4.5	111	37.7	154	41.9	82.7	9.25	35.4	7.4	1.3	5.93	0.98	6.12	1.29	3.63	0.56	3.88	0.62
ns1	33.15	60.37	18.13	6.36	2.38	0.80	1.86	4.05	0.91	0.17	0.09	4.5	99.73	47.9	693	76.4	30.0	5.2	24.6	186.4	17	130	18.9	4.4	113	34.7	165	43.1	85.1	9.16	35.4	7.2	1.2	5.83	0.98	5.62	1.11	3.28	0.55	3.53	0.51
ns1	33.98	58.67	18.95	6.59	2.50	0.75	1.63	4.44	0.92	0.16	0.09	5.1	99.90	41.1	751	16.4	29.5	5.3	27.3	201.6	17	131	17.4	4.0	110	35.9	156	43.3	85.8	9.50	36.5	7.6	1.3	6.09	0.99	5.83	1.23	3.27	0.57	3.57	0.55
ns1	34.72	57.19	19.60	6.38	2.51	0.77	1.60	5.04	0.98	0.15	0.09	5.5	99.92	65.0	746	22.8	40.6	5.5	27.7	229.0	18	151	21.3	5.1	131	36.8	182	45.6	91.1	9.80	36.6	7.5	1.2	5.96	1.05	5.96	1.23	3.65	0.61	4.18	0.67
ns1	36.70	59.35	18.79	6.04	2.39	0.72	1.75	4.44	0.98	0.15	0.08	5.0	99.79	44.5	675	17.2	34.4	5.3	25.5	206.9	18	132	20.1	5.4	122	33.3	178	46.4	90.2	9.97	35.8	7.1	1.2	5.37	0.94	5.68	1.15	3.36	0.58	3.52	0.59
ns1	37.54	62.37	16.59	6.29	2.21	0.78	2.05	3.74	0.83	0.15	0.09	4.7	99.90	51.3	639	42.3	25.0	5.8	25.2	173.7	14	136	19.2	4.6	108	37.6	172	46.5	91.8	10.31	38.9	8.0	1.4	6.44	1.07	6.59	1.28	3.42	0.56	3.70	0.58
ns1	38.71	57.71	19.70	6.14	2.49	0.69	1.65	4.83	0.95	0.16	0.09	5.3	99.82	51.3	775	21.4	29.6	5.6	26.7	221.3	18	132	20.4	5.0	120	32.6	158	46.6	91.6	9.82	35.0	6.7	1.2	5.40	0.91	5.60	1.13	3.14	0.53	3.63	0.59
ns1	39.64	61.97	17.22	6.25	2.25	0.77	1.96	4.04	0.84	0.15	0.09	4.3	99.93	30.8	682	19.6	24.9	5.2	25.6	180.0	14	142	17.6	4.7	100	36.3	165	40.5	79.8	9.02	34.8	7.1	1.3	6.23	1.06	6.60	1.25	3.46	0.57	3.65	0.58
ns1	40.49	58.48	19.14	6.55	2.48	0.69	1.69	4.80	1.01	0.17	0.09	4.7	99.90	41.1	732	18.5	31.4	4.8	23.6	212.6	19	139	22.2	5.8	137	35.1	170	42.6	89.0	9.07	35.4	7.4	1.3	5.79	1.10	5.54	1.18	3.60	0.59	3.78	0.71
ns1	41.24	58.68	19.14	6.53	2.52	0.64	1.44	5.00	0.86	0.14	0.09	4.8	99.94	27.4	761	20.2	32.3	4.9	25.6	232.1	18	145	19.7	4.6	132	35.1	140	39.9	82.8	8.92	35.1	7.3	1.2	5.66	0.96	5.65	1.27	3.68	0.59	3.70	0.59
ns1	42.18	61.65	17.28	6.39	2.39	0.74	1.84	4.12	0.93	0.18	0.10	4.2	99.91	17.1	682	26.2	36.8	5.4	24.5	186.8	16	140	17.9	5.0	121	37.2	171	48.9	101.2	10.55	41.7	8.4	1.4	6.37	1.08	5.84	1.30	3.82	0.63	3.77	0.64
ns1	43.52	58.48	19.06	6.53	2.52	0.71	1.61	4.84	0.94	0.16	0.09	4.9	99.93	20.5	736	19.9	34.0	4.6	25.2	228.3	17	154	19.4	5.2	127	36.7	155	49.0	101.0	10.63	42.8	8.2	1.4	6.33	1.07	5.85	1.29	3.79	0.63	3.92	0.59
ns1	45.00	57.95	19.48	6.83	2.55	0.58	1.54	4.85	0.91	0.16	0.09	4.9	99.94	20.5	748	18.9	33.1	4.0	27.8	218.3	18	134	19.2	4.5	131	33.1	145	42.7	84.0	8.84	35.0	7.2	1.1	5.48	0.96	5.40	1.20	3.66	0.52	3.53	0.61
ns1	45.71	60.11	18.01	6.67	2.37	0.84	1.87	4.26	0.96	0.18	0.10	4.4	99.87	37.6	711	45.3	33.4	6.1	27.0	198.5	17	149	20.4	5.7	130	42.7	185	43.9	91.8	9.92	40.8	8.4	1.5	7.32	1.24	7.15	1.56	4.42	0.73	4.47	0.64
ns1	46.82	58.64	19.14	6.45	2.59	0.70	1.57	4.95	0.94	0.14	0.10	4.6	99.91	34.2	720	21.7	36.9	4.8	26.9	244.5	19	151	22.5	5.0	144	38.9	163	54.2	109.6	11.40	44.5	8.4	1.5	5.77	1.02	6.05	1.21	3.59	0.58	3.85	0.66
ns1	47.62	57.41	20.28	6.38	2.54	0.36	1.17	5.63	0.76	0.11	0.08	5.0	99.82	41.1	730	107.7	30.1	3.6	26.6	267.7	19	116	15.6	4.3	146	22.8	118	31.4	66.1	6.66	26.2	5.1	0.7	3.43	0.61	3.37	0.83	2.45	0.37	2.67	0.48
ns1	48.84	56.13	20.55	6.96	2.66	0.52	1.16	5.40	0.83	0.13	0.09	5.4	99.93	17.1	762	20.8	28.4	4.4	26.0	273.9	20	157	22.2	4.2	152	33.6	137	34.4	71.6	7.59	30.7	6.2	1.0	5.21	0.87	5.03	1.16	3.53	0.59	3.61	0.63
ns1	49.74	61.11	17.37	6.52	2.46	0.68	1.80	4.22	0.91	0.17	0.10	4.5	99.92	13.7	681	23.7	35.5	5.5	31.3	201.0	16	143	18.2	4.5	125	36.0	171	46.5	94.2	9.86	39.8	7.4	1.3	6.06	0.96	5.55	1.25	3.68	0.59	3.61	0.68
ns1	50.33	59.19	18.46	6.63	2.56	0.57	1.57	4.55	0.91	0.17	0.10	5.1	99.91	27.4	703	21.4	41.6	4.6	31.5	219.2	17	134	17.8	4.2	125	30.8	162	46.2	94.4	9.94	39.1	6.9	1.1	4.87	0.91	4.88	1.11	3.31	0.56	3.34	0.58
ns1	51.22	57.88	19.37	6.91	2.65	0.51	1.44	5.00	0.82	0.14	0.10	5.0	99.91	34.2	741	18.6	31.5	4.0	28.0	235.7	18	147	17.9	4.0	132	28.7	134	36.9	77.5	8.11	32.3	6.0	1.0	4.87	0.76	4.33	0.97	2.95	0.52	2.76	0.58
ns1	53.17	60.64	17.83	6.32	2.55	0.60	1.85	4.44	0.91	0.16	0.10	4.4	99.90	44.5	725	44.0	35.5	4.8	29.2	206.5	17	137	18.4	4.1	123	33.3	161	42.7	90.5	9.29	37.5	7.5	1.1	6.12	0.89	5.11	1.12	3.46	0.49	3.16	0.55
ns1	55.26	62.76	16.53	6.30	2.34	0.62	2.05	3.76	0.80	0.14	0.10	4.4	99.89	30.8	652	69.7	25.1	4.5	29.1	177.3	14	132	16.1	3.8	112	31.2	143	43.8	89.9	9.41	37.4	6.7	1.2	5.75	0.97	5.20	1.09	3.19	0.54	2.90	0.49
ns1	56.10	62.88	16.59	6.07	2.31	0.70	2.00	3.85	0.86	0.18	0.09	4.3	99.91	20.5	661	25.3	35.2	4.7	26.4	187.4	15	140	18.2	4.6	113	32.6	167	46.8	95.9	9.87	41.5	8.3	1.3	5.83	0.95	5.41	1.14	3.28	0.50	3.27	0.54
ns1	58.31	54.71	21.88	5.81	2.45	0.38	1.15	6.03	0.78	0.14	0.07	6.4	99.91	17.1	905	18.5	49.7	5.5	24.0	295.1	21	206	22.2	5.1	146	50.7	165	37.2	75.4	7.95	34.7	7.2	1.1	6.40	1.25	7.94	1.71	5.23	0.87	4.62	0.74
ns1	59.46	57.99	20.15	6.09	2.43	0.32	1.28	5.16	0.80	0.16	0.07	5.4	99.95	37.6	805	19.8	38.1	4.4	24.3	245.9	18	165	19.5	3.6	130	33.5	138	34.9	72.2	7.69	30.0	6.0	0.8	5.09	0.84	5.08	1.19	3.58	0.57	3.51	0.60
ns1	60.35	59.75	18.92	6.09	2.32	0.35	1.44	4.87	0.85	0.17	0.07	5.0	99.92	41.1	730	38.2	22.5	3.8	26.7	228.3	17	138	19.3	4.7	125	30.0	127	40.0	81.3	8.79	33.5	6.3	1.1	5.09	0.87	4.48	0.98	2.94	0.44	3.02	0.47
ns1	61.00	61.06	18.01	6.20	2.30	0.35	1.60	4.52	0.84	0.17	0.07	4.6	99.82	37.6	709	19.1	34.5	4.4	26.8	217.5	16	145	17.5	4.0	117	31.3	138	40.2	81.5	8.63	34.7	6.9	1.0	5.08	0.88	4.94	1.08	3.21	0.53	3.14	0.51
ns1	61.90	64.26	15.92	5.78	2.01	1.10	1.84	3.63	0.84	0.25	0.08	4.1	99.89	23.9	635	19.2	36.5	4.4	25.5	156.3	14	145	14.7	3.5	87	52.9	151	48.5	99.7	10.74	46.1	10.3	1.8	9.42	1.51	8.38	1.76	4.85	0.75	3.82	0.60
ns1	63.18	60.11	18.22	6.88	2.43	0.32	1.47	4.64	0.79	0.12	0.08	4.8	99.96	23.9	728	17.5	31.4	3.9	27.6	222.0	16	147	18.4	3.9	117	29.4	128	41.1	83.6	8.81	33.7	7.5	1.1	5.05	0.86	4.97	1.06	3.02	0.46	3.03	0.51
ns1	64.30	59.64	18.34	6.50	2.40	0.50	1.49	4.64	0.81	0.26	0.08	5.2	99.96	44.5	734	19.7	35.8	3.8	25.2	222.9	17	151	18.9	4.1	125	37.7	130	54.5	110.3	11.62	48.9	10.6	1.9	8.43	1.28	6.05	1.27	3.51	0.56	3.27	0.52
ns1	65.26	56.24	21.38	5.84	2.42	0.42	1.39	5.64	0.70	0.11	0.06	5.6	99.92	17.1	934	21.5	40.1	4.5	26.7	282.8	18	232	22.0	5.3	136	39.8	149	35.3	73.8	7.69	31.7	6.2	1.0	5.48	1.10	6.14	1.39	3.94	0.63	3.76	0.60
ns1	66.20	57.63	20.13	6.48	2.46	0.40	1.67	5.05	0.62	0.12	0.07	5.2	99.94	20.5	914	26.5	40.6	3.8	26.2	260.6	17	223	19.4	4.6	127	26.1	122	24.6	50.2	5.29	20.7	4.3	0.7	3.48	0.61	3.93	0.87	2.81	0.46	2.69	0.45
ns1	66.66	60.46	18.47	6.25	2.37	0.34	1.60	4.71	0.72	0.13	0.07	4.7	99.91	20.5	768	15.5	35.5	4.1	22.5	234.2	16	178	18.6	4.0	115	31.0	124	37.3	75.9	8.23	32.7	7.1	1.1	5.52	0.89	5.31	1.11	3.23	0.52	3.14	0.51
ns1	69.08	59.20	19.45	5.87	2.43	0.38	1.67	4.97	0.67	0.12	0.07	5.0	99.94	27.4	851	12.2	44.2	3.9	19.8	247.5	16	214	17.4	4.8	123	31.0	118	37.6	78.1	8.15	31.5	5.6	1.0	4.41	0.79	5.05	1.02	3.06	0.49	3.04	0.42
ns1	69.32	58.93	19.01	6.70	2.50	0.42	1.60	4.80	0.66	0.14	0.08	5.0	99.95	27.4	825	21.5	41.2	3.7	28.3	244.8	16	214	17.7	4.0	126	23.4	120	24.8	49.8	4.95	20.3	4.0	0.8	2.97	0.51	3.47	0.77	2.58	0.41	2.46	0.46
ns1	70.00	59.31	18.19	7.35	2.71	0.36	1.56	4.64	0.67	0.13	0.09	4.8	99.91	34.2	733	20.2	41.3	3.1	30.0	227.7	15	171	16.3	3.9	114	23.5	99	34.7	70.0	7.29	29.2	5.6	1.0	3.91	0.67	3.77	0.85	2.33	0.38	2.38	0.39
ns1	70.36	59.03	19.66	5.66	2.37	0.41	1.70	5.00	0.70	0.11	0.06	5.1	99.91	34.2	871	10.9	41.6	3.9	17.9	249.8	17	215	20.1	4.8	127	36.8	135	41.5	83.4	8.88	35.6	7.6	1.1	5.46	0.96	5.67	1.20	3.89	0.61	3.45	0.56
ns1	71.91	60.53	19.19	5.27	2.27	0.39	1.47	5.06	0.74	0.14	0.06	4.7	99.93	27.4	827	12.4	29.8	4.4	19.6	264.6	18	201	20.6	5.5	134	31.5	151	52.2	105.8	10.77	43.3	8.6	1.6	5.87	0.98	4.80	1.10	3.41	0.52	3.55	0.61
ns1	72.78	59.31	18.97	5.83	2.39	0.73	1.31	5.09	0.73	0.45	0.07	4.9	99.89	27.4	811	13.4	38.7	4.0	22.2	264.8	18	211	21.2	5.1	125	119.0	135	108.8	212.9	23.04	99.3	21.6	4.7	21.79	3.47	19.4	3.87	9.42	1.18	6.55	0.97
ns1	73.36	58.69	19.52	5.91	2.31	0.35	1.18	5.56	0.73	0.10	0.06	5.3	99.81	20.5	845	17.1	43.5	5.1	22.0	278.4	18	204	24.8	4.1	141	49.0	149	50.6	92.3	10.54	38.8	7.7	1.5	6.87	1.22	8.60	1.84	4.68	0.59	4.34	0.61
ns1	74.59	58.54	18.59	7.25	2.55	0.31	1.23	4.94	0.79	0.12	0.08	5.3	99.80	54.7	737	28.0	34.7	4.4	29.7	247.7	18	157	18.3	4.0	130	34.2	128	46.1	83.3	9.57	35.2	7.1	1.3	5.88	0.93	6.14	1.27	3.53	0.53	3.59	0.49
ns1	76.28	54.47	20.56	8.34	2.73	0.67	0.86	5.35	0.69	0.36	0.09	5.6	99.83	27.4	813	16.7	39.9	3.2	32.5	253.4	18	182	19.4	4.7	137	36.9	117	54.4	94.1	11.49	46.7	10.3	2.1	7.93	1.19	6.81	1.17	3.27	0.46	3.16	0.47
ns1	76.65	55.36	21.06	7.46	2.58	0.28	0.91	5.67	0.72	0.11	0.07	5.5	99.83	30.8	816	25.2	37.9	3.7	28.6	276.3	19	180	21.1	5.0	134	35.3	129	45.9	81.4	9.28	34.8	6.8	1.2	4.90	0.89	5.85	1.29	3.43	0.45	3.74	0.49
ns1	78.45	51.83	23.25	6.79	2.68	0.30	1.12	6.46	0.98	0.12	0.07	6.1	99.81	44.5	875	17.1	42.7	4.9	23.4	306.5	23	178	26.3	6.9	183	31.3	171	53.3	91.0	10.37	39.0	7.4	1.3	5.48	0.91	5.43	1.19	3.42	0.63	3.92	0.58
ns1	80.89	56.28	20.94	5.92	2.34	0.35	1.89	5.37	1.17	0.18	0.06	5.2	99.80	30.8	776	25.3	31.3	6.3	25.6	248.6	22	162	25.6	7.1	155	35.8	221	60.7	105.9	11.63	44.1	9.3	1.3	6.69	0.97	6.55	1.26	3.95	0.58	4.27	0.65
ns1	81.51	48.25	25.12	6.27	2.67	1.10	1.02	7.09	1.15	0.13	0.08	6.8	99.81	41.1	1068	19.1	29.4	6.9	27.8	342.6	24	207	26.2	4.9	193	35.4	196	57.2	98.8	11.10	39.6	7.8	1.2	5.82	0.93	5.78	1.31	4.20	0.59	4.63	0.72
ns1	84.98	47.51	25.87	6.54	2.85	0.36	1.17	7.11	1.61	0.15	0.07	6.4	99.78	44.5	1111	23.8	31.6	9.6	27.6	338.3	32	167	36.6	8.1	236	52.9	304	61.7	107.1	12.09	45.9	9.1	1.3	7.56	1.22	9.17	1.93	5.79	0.86	6.23	0.96
ns1	89.99	49.13	24.27	7.41	3.06	0.34	1.11	6.70	1.17	0.17	0.09	6.2	99.78	44.5	978	23.2	44.1	6.6	34.8	331.5	25	195	30.6	7.7	174	47.3	204	67.2	118.1	13.26	47.5	9.2	1.4	7.16	1.14	8.10	1.70	4.93	0.80	5.24	0.84
ns1	90.93	64.91	16.17	5.89	1.89	0.39	3.02	2.64	0.74	0.18	0.08	3.8	99.78	27.4	579	30.9	29.3	6.4	24.0	117.3	12	158	16.4	5.1	100	40.1	197	54.6	98.5	11.22	42.3	8.2	1.5	6.37	1.12	7.87	1.50	3.87	0.62	3.64	0.48
ns1	95.00	61.61	16.56	6.20	2.20	0.41	2.93	2.97	1.14	0.18	0.09	5.4	99.77	27.4	656	39.5	60.6	8.3	30.4	129.2	18	161	24.3	6.8	132	52.6	291	45.1	82.2	9.41	34.7	7.3	1.3	6.75	1.20	9.14	1.93	5.57	0.80	5.14	0.70
ns1	95.49	50.70	22.15	6.72	2.89	0.48	1.84	5.52	1.98	0.25	0.09	7.0	99.75	58.2	882	46.8	97.6	13.2	39.3	276.1	30	180	45.4	10.6	227	80.8	433	87.0	154.9	17.36	65.7	12.8	2.2	11.24	1.88	13.9	3.03	8.43	1.23	7.51	1.16
ns1	96.38	53.12	22.14	7.16	2.91	0.38	1.76	5.29	1.23	0.19	0.09	5.4	99.79	37.6	893	23.4	41.9	7.0	30.5	257.3	24	181	26.8	6.2	184	56.2	228	65.5	114.3	13.09	47.8	10.0	1.6	8.34	1.50	9.86	2.07	5.82	0.87	5.87	0.77
ns1	98.35	54.50	21.67	6.48	2.69	0.38	1.95	5.42	1.10	0.19	0.09	5.2	99.79	34.2	911	22.5	39.8	6.7	27.9	238.4	22	175	23.0	5.5	149	54.3	208	68.1	121.5	13.72	51.4	9.6	1.9	8.97	1.44	9.25	2.11	5.36	0.79	5.10	0.73

Appendix A

Core	Stratigr level	SiO2 %	Al2O3 %	Fe2O3 %	MgO %	CaO %	Na2O %	K2O %	TiO2 %	P2O5 %	MnO %	LOI %	SUM %	Cr ppm	Ba ppm
ns1	99.70	50.99	22.64	6.87	2.91	0.49	1.74	5.72	1.42	0.21	0.09	6.5	99.71	51.3	895
ns1	100.28	51.66	23.33	6.61	2.93	0.38	1.25	6.26	1.18	0.18	0.08	5.8	99.79	44.5	998
ns1	101.50	50.38	24.30	6.27	2.90	0.31	1.17	6.72	1.19	0.13	0.07	6.2	99.77	41.1	1105
ns1	102.39	60.99	15.64	6.60	2.22	0.39	2.18	2.90	0.81	0.18	0.09	7.7	99.78	23.9	513
ns1	103.32	56.31	20.62	7.17	2.77	0.25	1.05	5.18	0.86	0.13	0.08	5.3	99.83	47.9	797
ns1	103.76	58.60	19.25	6.06	2.46	0.63	1.68	4.70	0.91	0.16	0.08	5.2	99.82	23.9	723
ns1	106.45	51.95	23.09	6.95	2.87	0.33	1.39	6.02	1.13	0.16	0.08	5.7	99.80	37.6	934
ns1	106.82	54.51	20.53	7.18	2.81	0.83	1.16	5.33	1.04	0.50	0.09	5.7	99.80	51.3	849
ns1	107.66	56.61	19.50	8.05	2.89	0.32	1.04	4.84	0.82	0.15	0.10	5.4	99.83	37.6	746
ns1	108.41	57.06	19.85	7.35	2.72	0.33	1.07	4.98	0.78	0.10	0.09	5.4	99.83	30.8	783
ns1	109.71	56.75	20.08	7.39	2.68	0.36	0.99	5.12	0.70	0.15	0.09	5.4	99.82	34.2	809
ns1	110.30	56.41	19.74	7.70	2.78	0.36	1.01	5.07	0.69	0.15	0.10	5.7	99.81	23.9	785
ns1	111.86	55.98	17.11	7.81	2.69	3.04	1.02	4.03	0.68	0.79	0.18	6.4	99.81	20.5	657
ns1	111.96	56.63	17.81	8.15	2.76	1.52	1.08	4.31	0.73	0.80	0.12	5.8	99.80	23.9	686
ns1	112.54	57.93	20.18	5.97	2.23	0.47	1.33	5.05	0.61	0.05	0.07	5.8	99.79	10.3	871
ns1	113.77	58.69	19.78	5.94	2.24	0.40	1.56	4.70	0.69	0.12	0.07	5.5	99.79	20.5	818
ns1	114.72	59.65	19.34	6.26	2.20	0.31	1.45	4.58	0.57	0.10	0.07	5.2	99.83	20.5	810
ns1	116.00	58.74	18.51	7.65	2.57	0.37	1.01	4.67	0.64	0.18	0.09	5.3	99.82	27.4	726
ns1	116.52	59.59	18.00	8.01	2.65	0.28	1.16	4.39	0.73	0.11	0.10	4.7	99.81	20.5	678
ns1	117.40	60.20	18.50	7.02	2.32	0.41	1.80	4.11	0.57	0.09	0.09	4.6	99.81	37.6	702
ns1	118.77	56.94	20.17	7.20	2.50	0.28	1.04	5.37	0.60	0.11	0.08	5.4	99.80	44.5	822
ns3	3.10	60.93	17.46	6.25	2.23	1.15	1.38	4.06	0.94	0.16	0.08	5.1	99.83	20.5	658
ns3	5.20	59.65	18.03	6.03	2.24	1.19	1.28	4.35	0.98	0.18	0.11	5.7	99.83	30.8	672
ns3	7.15	58.86	18.65	6.25	2.31	1.21	1.26	4.43	1.01	0.17	0.10	5.5	99.84	30.8	685
ns3	8.22	60.80	17.57	6.39	2.19	1.15	1.54	3.95	0.93	0.16	0.07	5.0	99.84	17.1	668
ns3	8.80	60.48	18.00	6.02	2.18	1.03	1.43	4.20	0.89	0.15	0.08	5.3	99.85	27.4	688
ns3	9.23	69.07	13.12	5.79	1.63	1.00	2.17	2.45	0.67	0.15	0.07	3.7	99.89	3.4	573
ns3	12.80	65.03	15.81	5.66	2.04	1.12	2.22	3.28	0.85	0.18	0.09	3.5	99.86	20.5	628
ns3	15.72	61.60	17.28	6.38	2.32	1.17	1.88	3.87	0.98	0.18	0.10	4.0	99.85	37.6	657
ns3	18.99	64.24	16.06	5.57	2.09	1.19	2.02	3.58	0.93	0.17	0.08	3.8	99.82	27.4	653
ns3	21.96	61.00	17.73	6.14	2.22	1.08	1.66	4.14	0.95	0.16	0.08	4.6	99.85	23.9	685
ns3	31.34	65.61	15.17	5.64	1.92	1.20	2.48	3.12	0.85	0.19	0.08	3.5	99.84	17.1	652
ns3	37.94	60.00	17.98	6.14	2.53	1.20	1.83	4.37	1.03	0.19	0.09	4.4	99.85	30.8	707
ns3	38.30	62.21	16.79	6.09	2.37	1.10	1.97	3.91	0.93	0.18	0.09	4.1	99.83	41.1	687
ns3	43.74	54.93	20.88	6.98	2.83	1.16	1.76	5.01	1.08	0.19	0.09	4.8	99.81	37.6	772
ns3	46.90	59.29	17.97	6.78	2.62	1.18	2.16	4.02	1.01	0.20	0.10	4.4	99.82	20.5	705
ns3	52.21	62.74	16.61	6.09	2.37	1.09	2.27	3.71	0.92	0.18	0.09	3.7	99.85	23.9	703
ns3	57.97	61.16	16.86	6.70	2.52	1.14	2.29	3.73	0.94	0.19	0.11	4.1	99.84	34.2	698
ns3	64.22	58.33	18.47	7.28	2.89	1.08	2.02	4.24	1.01	0.19	0.12	4.1	99.82	30.8	725
ns3	66.42	62.09	16.58	6.31	2.49	1.05	2.13	3.80	0.93	0.20	0.10	4.1	99.87	27.4	668
ns3	67.44	63.70	15.89	6.47	2.41	0.98	2.14	3.47	0.84	0.17	0.11	3.6	99.87	34.2	656
ns3	68.55	62.20	16.56	6.78	2.51	1.06	2.00	3.73	0.94	0.18	0.11	3.7	99.86	30.8	646
ns3	69.66	65.88	14.86	5.92	2.17	0.98	2.21	3.33	0.76	0.18	0.09	3.4	99.86	30.8	628
ns3	71.21	63.13	16.03	6.36	2.34	1.00	2.01	3.71	0.84	0.18	0.10	4.1	99.88	23.9	641
ns3	72.25	60.61	18.20	6.29	2.48	0.90	1.49	4.56	0.83	0.14	0.08	4.2	99.86	34.2	682
ns3	78.05	63.26	16.46	6.14	2.19	1.04	1.54	3.99	0.85	0.14	0.07	4.1	99.85	13.7	631
ns3	79.40	63.76	16.38	5.88	2.13	0.93	1.59	3.95	0.84	0.15	0.07	4.1	99.86	30.8	619
ns3	80.10	56.63	20.65	6.36	2.49	0.79	1.05	5.31	0.71	0.11	0.07	5.6	99.87	30.8	789
ns3	80.80	59.26	19.01	6.92	2.56	0.77	1.37	4.54	0.67	0.11	0.08	4.5	99.88	17.1	738
ns3	82.10	59.81	18.97	5.75	2.34	0.83	1.50	4.83	0.76	0.14	0.07	4.8	99.89	27.4	743
ns3	83.90	61.39	17.63	5.84	2.33	0.91	1.69	4.35	0.81	0.14	0.08	4.6	99.86	23.9	717
ns3	85.50	58.03	17.67	6.53	2.39	2.61	1.43	4.24	0.69	1.24	0.09	4.8	99.81	23.9	726
ns3	86.00	60.13	18.81	6.64	2.32	0.75	1.51	4.46	0.62	0.10	0.08	4.4	99.91	23.9	765
ns3	86.52	59.29	18.49	7.48	2.64	0.89	1.37	4.60	0.66	0.23	0.09	4.1	99.93	23.9	677
ns3	87.40	59.45	19.59	5.67	2.32	0.81	1.54	4.85	0.69	0.13	0.07	4.7	99.92	27.4	783
ns3	90.10	60.42	18.95	5.48	2.27	0.92	1.44	5.21	0.58	0.11	0.07	4.4	99.94	20.5	810
ns3	90.60	58.53	18.18	6.89	2.38	1.44	2.49	4.03	1.20	0.26	0.09	4.3	99.88	30.8	722
ns3	93.35	59.84	18.42	6.23	2.29	1.15	1.94	4.52	0.97	0.17	0.08	4.2	99.91	37.6	801
ns3	98.52	59.70	18.45	6.74	2.45	0.89	1.33	4.85	0.80	0.14	0.08	4.4	99.92	34.2	749
ns3	100.40	64.15	15.76	5.22	1.63	1.10	2.91	3.37	0.68	0.13	0.07	4.8	99.94	10.3	905
ns3	108.10	54.05	21.75	6.52	2.69	0.97	1.03	6.41	0.88	0.13	0.08	5.3	99.93	44.5	874
ns3	109.00	56.58	19.81	7.84	2.68	0.84	0.78	5.32	0.68	0.13	0.09	5.1	99.95	37.6	773
ns3	111.95	52.05	23.03	6.73	2.57	0.99	0.87	6.85	0.90	0.13	0.07	5.6	99.91	34.2	950
ns3	117.95	61.53	17.89	6.29	2.22	0.41	1.47	4.25	0.87	0.14	0.07	4.7	99.93	23.9	658
ns3	120.50	57.51	20.18	6.45	2.44	0.28	0.98	5.80	0.90	0.13	0.07	5.1	99.94	30.8	804
ns3	126.53	64.37	16.55	6.06	2.14	0.62	1.34	4.01	0.78	0.11	0.07	3.8	99.93	30.8	629
ns3	131.60	59.82	18.79	6.36	2.39	0.94	1.16	5.08	0.82	0.12	0.08	4.3	99.95	17.1	731
ns3	132.80	57.66	19.28	7.25	2.66	0.83	0.88	5.30	0.77	0.11	0.09	5.0	99.93	30.8	746
ns3	134.55	57.90	18.95	8.15	2.75	0.84	0.90	4.68	0.78	0.10	0.10	4.7	99.94	34.2	699
ns3	136.36	59.43	18.48	7.02	2.57	0.93	1.07	4.84	0.79	0.23	0.09	4.4	99.94	34.2	692
ns3	138.49	57.65	18.90	8.13	2.74	0.89	0.84	5.14	0.68	0.18	0.10	4.6	99.95	23.9	719
ns3	140.38	58.48	18.18	7.92	2.77	0.84	0.89	5.02	0.72	0.13	0.10	4.8	99.95	37.6	681
ns3	142.12	57.45	19.41	7.31	2.48	0.74	0.87	5.50	0.59	0.09	0.08	5.3	99.92	17.1	776
ns3	144.14	59.68	17.64	7.67	2.59	0.81	0.96	4.55	0.61	0.13	0.09	5.1	99.92	20.5	666
ns3	146.27	59.15	18.31	7.32	2.53	0.80	0.98	4.71	0.62	0.11	0.09	5.2	99.90	27.4	699
ns3	148.40	59.33	18.26	7.74	2.60	0.80	1.08	4.35	0.67	0.11	0.10	4.8	99.93	20.5	730

Core	Stratigr level	Co ppm	Cu ppm	Hf ppm	Ni ppm	Rb ppm	Sc ppm	Sr ppm	Th ppm	U ppm	V ppm	Y ppm	Zr ppm	La ppm	Ce ppm
ns1	99.70	194.8	63.7	8.0	138	269.6	28	182	29.0	8.1	219	61.0	273	70.8	125.8
ns1	100.28	25.8	41.3	6.8	34.5	320.1	22	178	27.6	6.1	164	44.7	199	68.4	124.7
ns1	101.50	18.8	36.1	6.0	26.7	309.0	25	161	28.1	7.2	185	40.5	186	64.7	113.3
ns1	102.39	44.1	109.3	8.2	37.1	140.3	15	160	21.2	9.3	116	49.6	236	54.3	99.9
ns1	103.32	21.1	35.0	4.4	29.8	269.0	19	152	22.4	5.1	148	39.8	133	51.0	91.1
ns1	103.76	29.6	48.2	5.4	30.9	232.1	19	175	22.8	7.4	138	49.1	176	55.5	100.4
ns1	106.45	24.5	40.3	7.0	30.8	302.9	24	169	28.9	7.4	186	37.0	207	64.8	117.4
ns1	106.82	28.2	41.0	5.5	31.8	271.6	21	168	27.7	6.5	164	108.2	176	107.4	191.4
ns1	107.66	23.4	38.0	4.4	32.3	254.9	18	151	21.5	5.3	144	31.4	130	47.7	86.2
ns1	108.41	22.2	55.0	4.5	29.8	261.8	19	169	24.0	5.7	147	62.0	137	49.3	90.3
ns1	109.71	44.6	41.0	4.2	38.3	275.9	18	179	19.0	4.0	135	32.6	122	53.3	95.1
ns1	110.30	19.7	44.2	3.8	27.8	256.4	18	174	22.3	4.3	138	24.8	117	39.2	70.5
ns1	111.86	21.1	38.1	3.3	31.2	222.2	15	253	18.2	6.1	122	102.6	106	94.4	162.5
ns1	111.96	30.8	40.7	3.4	32.6	229.9	16	240	21.0	5.5	130	83.0	106	98.1	174.3
ns1	112.54	29.5	42.2	4.5	28.4	237.1	17	201	20.7	5.4	119	26.9	147	34.7	62.6
ns1	113.77	19.6	53.0	4.5	20.6	231.9	17	206	21.3	4.1	117	25.9	144	39.7	73.0
ns1	114.72	15.1	36.0	3.8	17.7	226.6	15	210	18.1	4.6	114	25.2	134	46.1	85.0
ns1	116.00	26.7	36.7	3.6	30.4	241.7	16	141	18.6	5.0	132	17.5	100	31.0	63.5
ns1	116.52	23.1	50.7	4.1	29.5	237.6	17	133	20.5	5.4	138	26.4	112	39.6	79.2
ns1	117.40	31.0	33.4	3.7	26.1	214.8	15	169	17.5	4.7	136	21.3	115	29.6	58.7
ns1	118.77	16.8	39.0	4.4	23.8	306.7	18	177	20.1	5.2	153	30.8	129	37.1	75.5
ns3	3.10	12.0	33.2	5.2	27.0	209.8	16	80	18.5	3.1	122	39.6	163	20.1	55.5
ns3	5.20	18.0	36.3	5.0	25.2	223.0	17	74	18.4	4.1	129	40.5	167	58.4	154.0
ns3	7.15	17.2	33.8	6.1	27.0	246.3	18	78	18.1	4.7	138	45.2	181	43.4	110.2
ns3	8.22	10.0	39.1	5.8	23.1	213.7	16	97	18.0	5.1	132	40.1	180	30.2	56.2
ns3	8.80	12.3	22.5	5.6	22.2	228.7	16	87	17.0	4.2	129	35.0	157	28.2	71.1
ns3	9.23	8.5	22.7	5.8	17.3	114.9	9	121	13.0	2.6	70	39.4	189	32.1	56.4
ns3	12.80	15.7	25.7	6.7	22.1	164.6	13	112	17.3	4.0	103	40.3	201	33.2	68.2
ns3	15.72	13.4	31.9	5.5	23.8	206.6	16	105	18.3	6.2	132	40.6	193	39.9	79.9
ns3	18.99	14.9	36.3	7.4	22.3	188.3	15	110	18.9	4.7	111	41.0	222	40.8	84.0
ns3	21.96	12.8	27.4	6.4	22.3	228.4	17	93	18.3	4.1	137	41.8	186	34.2	70.1
ns3	31.34	18.3	35.0	6.7	26.4	159.8	12	137	16.2	4.9	96	42.3	227	42.1	85.0
ns3	37.94	13.8	40.3	5.9	22.2	252.7	17	127	21.6	5.4	141	46.7	193	44.6	89.0
ns3	38.30	12.9	32.3	5.6	21.2	209.1	15	123	18.9	5.4	118	39.8	178	29.9	62.8
ns3	43.74	17.5	32.9	6.5	25.7	292.5	20	151	22.2	5.4	165	43.6	190	29.6	60.4
ns3	46.90	17.3	39.2	7.3	29.4	223.6	16	161	20.7	5.8	132	45.1	211	38.3	75.3
ns3	52.21	13.4	24.0	5.9	23.3	190.0	15	157	16.2	4.0	117	38.7	183	39.0	77.0
ns3	57.97	15.2	26.4	6.2	28.4	193.0	15	164	18.6	5.1	124	41.3	201	48.1	93.3
ns3	64.22	14.6	28.6	6.2	30.7	242.7	18	138	19.0	5.6	144	40.6	188	46.4	90.0
ns3	66.42	12.6	34.0	6.2	26.0	201.0	15	153	18.2	4.9	129	39.0	185	41.0	83.0
ns3	67.44	13.6	29.7	5.2	26.4	185.7	13	151	16.5	4.3	117	36.7	166	40.1	80.1
ns3	68.55	14.7	24.4	5.8	28.3	190.5	15	139	19.7	5.0	130	39.0	175	59.0	111.3
ns3	69.66	15.1	34.4	4.9	28.8	165.2	12	149	13.6	3.5	101	35.3	158	34.2	68.8
ns3	71.21	14.0	31.1	5.3	25.2	184.7	14	142	17.1	3.8	114	35.5	159	37.5	75.3
ns3	72.25	12.7	31.6	4.6	23.1	251.8	17	147	18.3	4.6	135	35.5	137	31.2	64.6
ns3	78.05	14.3	42.1	5.1	24.2	216.9	15	149	18.3	5.5	118	37.8	164	39.3	77.9
ns3	79.40	13.4	32.5	5.0	20.2	218.9	14	146	17.9	4.6	120	38.3	151	34.5	69.6
ns3	80.10	16.2	40.3	4.9	21.5	313.1	19	187	20.9	5.0	143	36.5	140	32.7	67.0
ns3	80.80	13.6	41.2	3.6	21.5	239.7	17	170	18.7	4.2	122	28.5	104	33.9	72.4
ns3	82.10	9.4	32.9	4.4	18.9	269.1	17	169	19.5	5.3	136	31.8	120	32.1	64.5
ns3	83.90	12.5	37.2	4.5	20.8	238.2	16	180	20.0	4.5	125	32.3	125	33.1	66.7
ns3	85.50	13.5	37.2	4.2	22.0	233.7	16	247	19.7	6.5	115	62.7	117	86.4	166.1
ns3	86.00	8.5	40.0	4.0	17.2	224.9	16	183	16.5	4.0	126	28.5	129	34.1	70.8
ns3	86.52	15.0	37.1	2.9	24.6	245.0	16	163	16.2	4.9	119	29.6	98	38.8	85.6
ns3	87.40	9.8	46.2	4.5	19.1	250.7	17	182	18.5	3.7	133	34.6	141	37.7	75.7
ns3	90.10	10.2	21.0	6.0	16.1	249.8	11	224	27.6	7.1	71	35.1	171	47.6	108.8
ns3	90.60	18.5	32.2	7.9	28.0	191.6	21	171	24.1	5.5	148	50.8	291	56.6	113.7
ns3	93.35	12.6	30.7	6.7	21.5	220.0	17	157	17.1	4.7	128	43.4	218	44.1	87.8
ns3	98.52	12.5	36.0	4.7	23.5	249.1	17	143	22.6	3.2	139	37.5	146	36.4	78.7
ns3	100.40	17.0	67.2	7.2	23.2	148.1	11	219	14.0	6.1	102	37.9	222	33.2	74.5
ns3	108.10	8.0	45.3	4.8	19.9	314.9	24	142	24.2	3.9	191	38.1	165	35.8	77.0
ns3	109.00	14.2	35.6	4.4	26.4	279.8	19	126	19.4	4.2	149	33.8	129	40.4	83.2
ns3	111.95	12.6	34.9	5.2	22.1	312.1	22	138	23.2	3.6	175	42.3	160	39.8	84.1
ns3	117.95	11.7	33.5	5.1	21.6	208.3	17	122	18.6	5.6	126	28.9	162	45.9	94.1
ns3	120.50	11.6	33.8	5.1	23.2	289.7	19	131	21.9	5.5	159	28.2	153	46.5	93.2
ns3	126.53	12.2	28.8	4.0	22.7	197.9	14	111	18.6	3.4	114	32.8	136	44.4	93.9
ns3	131.60	11.0	34.3	5.0	23.9	254.9	17	131	18.3	3.7	145	34.8	144	40.6	83.7
ns3	132.80	13.4	39.9	5.2	27.0	267.7	19	130	18.1	3.6	152	35.8	128	41.2	83.2
ns3	134.55	16.1	41.5	3.5	29.8	243.1	18	113	20.2	4.0	142	34.2	120	43.5	84.8
ns3	136.36	15.4	33.9	4.7	24.0	241.2	17	123	17.7	4.4	140	41.0	126	43.8	89.5
ns3	138.49	25.4	38.3	3.6	30.1	266.2	18	144	21.3	4.1	149	33.0	116	38.7	78.0
ns3	140.38	16.1	45.0	4.4	31.0	263.2	17	146	16.8	4.8	149	31.8	116	39.5	78.2
ns3	142.12	9.8	38.2	4.9	21.4	276.7	17	172	21.9	3.9	144	31.8	140	39.6	74.9
ns3	144.14	17.9	43.9	3.4	24.4	239.0	16	141	19.9	3.9	133	26.6	108	34.2	64.3
ns3	146.27	9.3	44.8	3.4	22.2	248.2	16	151	19.3	1.9	133	28.4	113	45.2	85.9
ns3	148.40	20.8	40.5	3.5	28.0	231.9	16	145	22.8	3.2	131	29.7	120	38.8	78.9

Core	Stratigr level	Pr ppm	Nd ppm	Sm ppm	Eu ppm	Gd ppm	Tb ppm	Dy ppm	Ho ppm	Er ppm	Tm ppm	Yb ppm	Lu ppm
ns1	99.70	13.85	49.6	10.4	1.8	9.29	1.56	10.5	2.24	6.17	0.97	5.73	0.94
ns1	100.28	13.73	51.9	9.6	1.7	7.75	1.36	8.06	1.71	4.64	0.78	4.83	0.76
ns1	101.50	12.56	46.2	8.8	1.4	7.49	1.25	7.15	1.50	4.60	0.73	5.02	0.76
ns1	102.39	11.46	45.2	9.1	1.7	8.99	1.47	9.86	1.84	5.03	0.76	5.01	0.70
ns1	103.32	10.35	38.4	8.1	1.4	6.90	1.11	6.89	1.42	4.01	0.60	3.84	0.62
ns1	103.76	11.39	40.3	9.1	1.6	7.59	1.27	8.71	1.71	4.84	0.70	4.38	0.59
ns1	106.45	13.35	47.9	9.8	1.6	7.35	1.10	6.91	1.44	3.80	0.69	4.79	0.68
ns1	106.82	22.73	87.4	20.1	3.6	17.06	2.80	18.5	3.83	9.57	1.21	7.59	1.04
ns1	107.66	9.96	37.1	8.3	1.5	6.34	0.90	5.93	1.10	3.22	0.42	3.41	0.54
ns1	108.41	10.34	37.8	8.1	1.5	8.10	1.50	10.3	2.00	5.52	0.80	4.87	0.63
ns1	109.71	11.26	41.7	8.2	1.6	6.07	0.96	5.72	1.14	3.15	0.50	3.23	0.50
ns1	110.30	7.80	28.8	6.3	1.1	4.30	0.72	4.40	0.90	2.78	0.40	3.01	0.45
ns1	111.86	20.42	87.0	21.9	5.1	21.12	3.00	18.0	3.31	7.76	1.03	5.46	0.75
ns1	111.96	20.78	87.4	21.1	4.7	19.22	2.67	15.6	2.74	6.35	0.85	4.86	0.64
ns1	112.54	7.04	25.7	5.1	0.9	3.68	0.68	3.98	0.94	3.29	0.47	3.39	0.50
ns1	113.77	8.18	28.0	5.4	0.9	3.82	0.67	4.45	0.97	2.99	0.48	3.31	0.48
ns1	114.72	9.54	35.3	6.9	0.9	5.25	0.76	5.02	0.97	2.62	0.41	2.67	0.44
ns1	116.00	6.73	27.0	5.1	0.8	3.05	0.60	3.28	0.75	2.21	0.36	2.23	0.40
ns1	116.52	8.53	32.9	6.9	0.8	4.94	0.93	5.30	1.10	3.27	0.52	2.93	0.47
ns1	117.40	6.27	24.2	4.4	0.6	3.55	0.65	3.88	0.89	2.48	0.42	2.97	0.47
ns1	118.77	8.04	32.0	6.4	1.1	4.52	0.83	5.01	1.28	3.22	0.50	3.08	0.49
ns3	3.10	5.80	29.1	7.0	1.3	6.14	1.45	6.39	1.33	3.61	0.57	3.98	0.63
ns3	5.20	11.05	46.3	8.2	1.5	6.41	1.71	6.39	1.28	3.67	0.63	3.83	0.63
ns3	7.15	9.66	41.5	8.9	1.5	6.87	1.73	7.24	1.46	4.15	0.64	4.18	0.69
ns3	8.22	7.57	33.0	7.3	1.4	6.30	1.55	6.69	1.22	3.83	0.60	3.81	0.63
ns3	8.80	7.26	29.3	7.4	1.2	5.76	1.31	5.39	1.15	3.49	0.57	3.51	0.50
ns3	9.23	8.25	36.6	9.5	1.6	6.48	1.63	6.84	1.26	3.60	0.51	3.23	0.53
ns3	12.80	7.51	33.1	6.6	1.4	6.22	1.58	6.25	1.35	3.78	0.62	3.71	0.52
ns3	15.72	8.37	34.5	7.7	1.3	6.30	1.48	6.26	1.34	4.10	0.64	3.88	0.62
ns3	18.99	8.73	38.2	7.5	1.4	7.03	1.58	6.35	1.31	3.94	0.61	3.89	0.63
ns3	21.96	7.63	33.8	7.7	1.4	6.32	1.51	6.56	1.30	4.13	0.63	4.26	0.66
ns3	31.34	9.33	40.8	9.3	1.6	7.32	1.80	7.28	1.36	4.17	0.67	4.08	0.58
ns3	37.94	9.43	40.2	8.3	1.6	7.62	1.74	7.55	1.49	4.45	0.71	4.47	0.67
ns3	38.30	6.86	29.8	7.3	1.3	5.84	1.48	6.41	1.28	3.98	0.57	3.81	0.59
ns3	43.74	7.08	30.2	7.1	1.4	6.48	1.72	7.39	1.47	4.32	0.70	4.31	0.70
ns3	46.90	8.32	35.6	8.9	1.7	7.30	1.77	7.79	1.48	4.60	0.71	4.29	0.74
ns3	52.21	7.97	33.1	6.6	1.3	6.47	1.51	6.32	1.19	3.94	0.61	3.86	0.58
ns3	57.97	10.40	40.3	8.0	1.6	6.53	1.60	6.93	1.29	4.09	0.61	3.82	0.56
ns3	64.22	9.39	37.0	6.8	1.4	6.18	1.53	6.45	1.32	3.92	0.58	4.24	0.68
ns3	66.42	8.85	33.9	7.5	1.3	6.44	1.47	6.71	1.34	4.01	0.56	4.20	0.62
ns3	67.44	9.19	34.9	7.0	1.4	5.87	1.47	6.61	1.33	3.76	0.54	3.45	0.60
ns3	68.55	11.45	42.7	7.7	1.3	6.18	1.51	6.66	1.20	3.84	0.61	3.83	0.63
ns3	69.66	7.97	32.9	7.1	1.2	6.11	1.36	5.90	1.16	3.43	0.54	3.50	0.49
ns3	71.21	8.33	33.5	6.5	1.4	5.37	1.30	5.97	1.15	3.37	0.51	3.42	0.56
ns3	72.25	7.42	29.9	6.9	1.2	5.92	1.45	5.65	1.15	3.22	0.54	3.50	0.51
ns3	78.05	8.93	36.8	7.3	1.6	6.44	1.57	6.64	1.30	3.86	0.60	3.35	0.51
ns3	79.40	8.29	33.6	7.3	1.3	6.30	1.52	6.11	1.29	3.62	0.52	3.67	0.58
ns3	80.10	7.87	32.3	6.0	1.2	5.65	1.38	5.84	1.18	3.45	0.52	3.33	0.55
ns3	80.80	7.73	29.3	5.7	1.0	4.65	1.15	4.96	0.97	2.68	0.47	2.70	0.45
ns3	82.10	7.22	28.5	6.0	1.0	4.87	1.26	4.90	1.04	3.13	0.47	3.13	0.48
ns3	83.90	7.93	29.2	5.8	1.2	5.17	1.33	5.80	1.11	3.38	0.49	3.21	0.50
ns3	85.50	19.38	80.1	14.9	2.6	13.53	2.51	9.72	1.81	4.75	0.65	4.43	0.71
ns3	86.00	7.39	31.2	5.2	1.1	4.96	0.85	5.31	0.87	2.64	0.41	3.29	0.47
ns3	86.52	8.70	36.9	7.6	1.2	5.55	0.88	5.55	0.98	2.67	0.35	3.16	0.44
ns3	87.40	7.89	33.3	7.6	1.1	5.27	0.92	5.42	1.19	3.01	0.51	4.36	0.64
ns3	90.10	11.13	48.9	9.8	1.3	8.71	1.23	6.01	1.23	3.02	0.51	4.18	0.60
ns3	90.60	11.60	51.1	9.0	1.8	10.88	1.34	8.72	1.80	4.44	0.78	5.47	0.79
ns3	93.35	10.30	41.5	7.7	1.6	7.03	1.13	7.60	1.48	4.31	0.60	5.06	0.66
ns3	98.52	8.68	35.9	6.8	1.4	8.10	1.21	6.44	1.33	3.39	0.54	3.98	0.49
ns3	100.40	7.45	36.0	8.3	1.4	7.61	1.03	7.14	1.16	3.66	0.53	3.84	0.56
ns3	108.10	8.33	38.4	5.0	1.3	6.66	1.00	6.65	1.24	3.76	0.66	5.07	0.72
ns3	109.00	9.31	36.3	6.7	1.2	6.80	1.12	6.79	1.26	3.68	0.46	3.57	0.67
ns3	111.95	8.98	36.4	6.9	1.7	8.25	1.28	6.96	1.53	4.29	0.62	4.53	0.68
ns3	117.95	9.85	38.4	6.1	1.3	6.75	0.82	6.13	0.94	2.80	0.47	3.64	0.57
ns3	120.50	9.85	41.6	7.9	1.6	6.55	0.84	5.32	0.96	2.58	0.50	4.21	0.65
ns3	126.53	9.95	41.3	6.3	1.6	7.88	1.16	6.64	1.21	3.12	0.56	3.51	0.45
ns3	131.60	9.06	37.6	7.1	1.4	7.31	1.05	6.11	1.43	3.38	0.56	4.14	0.61
ns3	132.80	9.65	41.4	6.7	1.5	6.09	0.91	5.34	1.36	3.48	0.55	3.86	0.59
ns3	134.55	9.74	39.8	7.3	1.2	6.55	0.88	6.49	1.21	3.37	0.44	3.82	0.55
ns3	136.36	10.10	41.0	6.9	1.2	7.63	1.11	6.78	1.41	3.65	0.55	4.23	0.56
ns3	138.49	8.80	40.2	7.8	1.3	6.92	0.86	5.48	1.20	3.28	0.42	3.26	0.57
ns3	140.38	8.88	36.0	6.8	1.4	6.73	0.97	6.21	1.18	3.31	0.47	3.93	0.51
ns3	142.12	8.35	34.0	5.1	1.3	5.51	0.95	6.01	1.05	3.15	0.55	3.78	0.63
ns3	144.14	7.32	29.9	4.2	1.4	4.73	0.77	5.33	0.89	2.69	0.36	3.01	0.46
ns3	146.27	9.26	36.9	5.1	1.2	5.19	0.73	4.99	1.03	2.99	0.52	3.16	0.47
ns3	148.40	8.52	34.3	5.9	1.2	6.49	0.90	5.62	1.07	2.75	0.49	4.52	0.51

Appendix A

Core	Stratigr level	SiO2	Al2O3	Fe2O3	MgO	CaO	Na2O	K2O	TiO2	P2O5	MnO	LOI	SUM	Cr	Ba	Co	Cu	Hf	Ni	Rb	Sc	Sr	Th	U	V	Y	Zr	La	Ce	Pr	Nd	Sm	Eu	Gd	Tb	Dy	Ho	Er	Tm	Yb	Lu
		%	%	%	%	%	%	%	%	%	%	%	%	ppm	ppm	ppm	ppm	ppm	ppm	ppm	ppm	ppm	ppm	ppm	ppm	ppm	ppm	ppm	ppm	ppm	ppm	ppm	ppm	ppm	ppm	ppm	ppm	ppm	ppm	ppm	ppm
ns3	149.26	58.37	18.64	7.88	2.73	0.79	0.99	4.82	0.67	0.13	0.10	4.7	99.92	27.4	733	29.3	42.3	4.8	28.5	255.4	16	146	20.9	4.2	135	29.7	126	42.8	77.4	9.16	37.5	6.0	1.2	5.87	0.82	5.95	1.14	2.77	0.42	3.43	0.52
ns3	150.40	57.96	19.51	6.44	2.62	0.83	1.20	5.23	0.75	0.11	0.08	5.1	99.93	30.8	749	10.1	41.4	4.6	20.5	266.2	18	132	19.5	4.6	146	34.4	139	44.0	86.6	9.38	38.3	5.8	1.3	5.52	0.92	5.84	1.12	3.06	0.53	4.64	0.59
ns4	1.63	68.52	14.16	5.38	1.73	1.21	2.03	2.97	0.66	0.15	0.07	3.0	99.95	13.7	523	10.8	22.4	4.5	19.8	143.2	10	128	14.4	3.7	88	33.9	181	44.6	80.5	9.82	44.1	7.5	1.5	6.13	0.94	6.31	1.21	3.20	0.46	3.81	0.51
ns4	3.25	68.86	14.03	5.37	1.77	1.30	1.92	2.86	0.65	0.14	0.07	2.9	99.94	6.8	552	11.1	21.1	5.6	19.3	134.7	10	154	14.9	5.8	80	33.5	222	36.9	73.4	8.64	37.0	5.9	1.4	5.46	1.02	5.79	1.18	2.94	0.45	3.74	0.52
ns4	5.37	64.13	15.96	6.24	2.20	1.19	1.61	3.30	0.76	0.18	0.09	4.2	99.93	23.9	584	10.3	25.3	4.6	23.0	159.5	13	114	16.2	5.4	98	32.1	185	40.2	79.2	8.86	34.1	5.5	1.1	5.52	0.85	5.63	1.18	3.12	0.46	2.97	0.51
ns4	7.28	66.01	14.95	5.59	2.10	1.35	1.82	3.46	0.81	0.18	0.08	3.5	99.92	27.4	538	15.8	32.4	6.1	23.6	170.1	13	117	22.1	4.0	107	42.3	245	47.0	93.9	10.37	43.6	8.4	1.9	8.43	1.26	7.18	1.29	3.85	0.58	4.77	0.59
ns4	10.05	67.02	14.45	5.67	1.96	1.29	1.91	3.18	0.73	0.16	0.08	3.4	99.93	27.4	542	10.9	28.1	6.2	20.2	157.3	11	133	17.1	3.7	97	36.4	197	43.7	90.4	9.84	40.6	6.9	1.4	7.60	1.21	6.73	1.35	3.60	0.48	4.00	0.62
ns4	12.00	64.21	16.06	5.84	2.08	1.08	1.77	3.64	0.80	0.15	0.09	4.1	99.90	30.8	610	14.5	32.1	5.7	26.4	177.2	13	146	15.8	4.0	105	38.3	170	47.1	90.8	10.60	41.0	8.1	1.4	6.35	1.18	6.63	1.33	3.43	0.59	3.99	0.57
ns4	14.10	60.25	18.51	6.08	2.33	1.21	1.58	4.43	0.97	0.16	0.09	4.2	99.90	41.1	643	13.7	30.7	5.9	24.8	218.4	17	161	21.9	5.2	136	42.2	191	52.5	103.0	11.76	45.1	8.5	1.5	6.94	1.21	6.86	1.53	3.98	0.65	4.17	0.66
ns4	16.17	63.54	17.02	5.73	2.06	1.11	1.81	3.90	0.88	0.19	0.09	3.5	99.91	23.9	647	13.9	32.1	5.8	21.5	190.6	14	165	19.0	4.4	110	42.8	186	51.7	102.2	11.57	43.3	8.8	1.5	7.35	1.20	6.53	1.49	4.05	0.59	4.04	0.62
ns4	17.51	58.77	18.89	6.37	2.40	1.15	1.56	4.52	0.93	0.13	0.10	5.0	99.92	27.4	684	14.2	40.7	6.1	28.5	223.1	17	173	22.4	4.5	136	40.5	188	48.2	93.3	10.86	40.2	7.9	1.5	6.93	1.02	6.30	1.40	3.64	0.63	3.90	0.64
ns4	18.17	66.26	15.00	5.64	1.86	1.03	2.07	3.14	0.72	0.14	0.09	3.9	99.92	23.9	599	12.0	26.7	5.6	23.6	147.1	11	177	15.4	4.6	85	40.5	189	46.2	88.4	10.18	40.2	7.4	1.5	6.95	1.06	6.31	1.43	3.54	0.54	3.34	0.51
ns4	20.80	62.69	17.03	6.03	2.23	1.11	1.83	3.87	0.84	0.19	0.10	3.9	99.90	20.5	639	12.9	32.4	5.5	25.3	182.6	15	172	16.8	4.3	107	36.4	174	43.6	84.1	9.80	38.6	7.0	1.4	6.29	1.05	5.78	1.27	3.63	0.57	3.74	0.56
ns4	27.93	58.89	18.49	6.52	2.48	1.29	1.98	4.20	0.98	0.16	0.11	4.7	99.89	27.4	701	17.6	36.3	7.2	31.1	207.6	17	192	21.8	4.8	131	43.6	228	59.7	114.1	12.71	45.0	8.4	1.5	6.99	1.15	7.03	1.54	4.11	0.67	4.63	0.66
ns4	31.20	61.16	17.68	5.97	2.21	1.22	2.04	4.13	0.92	0.20	0.09	4.2	99.90	20.5	662	14.4	29.6	6.0	26.2	191.3	15	191	21.3	4.5	115	40.8	221	52.0	96.1	10.60	41.6	6.9	1.4	6.28	1.04	6.26	1.45	3.92	0.66	4.07	0.67
ns4	33.38	65.22	15.51	5.85	2.02	1.09	2.17	3.33	0.78	0.18	0.09	3.6	99.92	17.1	624	13.0	21.3	6.2	24.0	148.9	12	173	15.7	3.9	91	37.7	192	45.7	89.3	9.88	38.1	6.4	1.3	5.87	1.00	5.75	1.23	3.30	0.56	3.69	0.55
ns4	34.81	63.64	16.16	5.77	2.08	1.13	1.99	3.72	0.86	0.18	0.09	4.2	99.90	27.4	636	13.8	28.3	6.5	25.4	171.5	14	180	20.0	3.2	102	38.5	206	52.4	100.0	11.37	42.5	8.1	1.5	7.01	1.12	6.80	1.31	3.60	0.56	3.81	0.59
ns4	37.08	62.08	17.22	5.92	2.13	1.13	1.82	4.06	0.92	0.18	0.08	4.3	99.92	20.5	627	13.2	26.8	5.6	25.5	189.5	15	180	18.7	6.3	111	42.3	198	51.8	98.8	11.24	42.1	7.5	1.4	6.92	1.18	7.09	1.46	3.83	0.62	4.03	0.67
ns4	39.20	60.26	18.24	6.05	2.16	1.13	1.79	4.31	0.95	0.16	0.08	4.7	99.91	23.9	686	12.2	29.5	6.0	25.1	198.4	17	170	22.9	5.0	114	41.7	189	48.7	93.5	10.16	39.1	6.8	1.4	6.63	1.12	6.35	1.41	3.96	0.65	4.37	0.71
ns4	40.65	61.40	17.29	6.11	2.25	1.21	1.98	3.98	0.91	0.20	0.09	4.4	99.91	47.9	674	19.5	47.0	5.9	30.0	193.8	15	189	21.1	5.6	113	42.3	204	54.3	104.6	11.80	43.4	8.1	1.3	7.01	1.12	6.64	1.50	3.86	0.62	4.07	0.68
ns4	44.31	65.34	15.33	5.44	1.85	1.13	2.34	3.24	0.78	0.18	0.09	4.1	99.90	23.9	630	13.7	30.8	5.7	24.0	153.9	12	183	16.7	4.6	96	36.7	214	46.3	88.4	10.26	38.1	6.9	1.5	6.08	1.03	6.09	1.28	3.60	0.53	3.82	0.57
ns4	46.73	60.01	18.25	6.41	2.32	1.22	2.07	4.23	0.95	0.17	0.10	4.1	99.92	27.4	697	14.9	31.9	6.7	26.3	205.4	17	191	19.1	5.9	127	41.6	208	51.3	99.5	11.06	41.4	8.6	1.5	6.38	1.01	6.62	1.52	3.89	0.60	4.19	0.66
ns4	54.85	59.66	18.31	6.35	2.40	1.14	1.69	4.43	0.91	0.15	0.09	4.7	99.92	34.2	636	14.2	35.1	5.4	25.6	233.4	17	186	24.4	5.2	138	40.6	186	47.8	91.7	10.40	39.7	7.5	1.4	6.72	1.09	6.41	1.43	3.95	0.52	4.09	0.64
ns4	62.14	55.33	20.62	6.75	2.64	1.34	1.75	5.01	1.11	0.16	0.10	5.0	99.90	34.2	696	14.7	33.9	7.1	28.7	256.7	21	186	27.2	6.3	153	46.3	212	56.2	104.7	11.52	41.7	8.8	1.7	7.02	1.15	6.99	1.53	4.35	0.61	4.58	0.70
ns4	64.88	65.06	15.51	5.80	2.02	1.21	2.32	3.28	0.77	0.17	0.09	3.6	99.91	23.9	595	15.8	29.7	7.1	23.9	149.0	12	191	17.6	4.4	94	36.6	214	44.3	87.7	10.13	38.8	7.9	1.2	6.20	1.01	6.35	1.30	3.67	0.50	3.32	0.54
ns4	68.93	61.63	17.17	5.99	2.40	1.12	1.72	4.21	0.86	0.16	0.09	4.5	99.93	27.4	615	15.4	37.6	6.0	27.7	221.9	15	185	21.1	4.2	120	38.9	182	48.9	97.9	10.81	40.5	7.8	1.5	6.65	1.11	6.30	1.35	3.56	0.53	3.94	0.57
ns4	75.03	59.48	18.22	6.56	2.55	1.28	2.15	4.23	0.94	0.20	0.11	4.1	99.91	37.6	656	17.2	37.3	6.3	35.7	214.9	17	185	19.7	5.8	140	39.5	218	56.5	108.7	12.15	44.1	8.6	1.5	6.39	1.14	6.78	1.44	3.46	0.54	3.90	0.60
ns4	78.90	65.10	15.36	6.06	2.20	1.13	2.38	3.27	0.76	0.17	0.11	3.3	99.92	34.2	591	13.4	22.7	5.9	24.1	151.6	13	186	14.6	3.9	100	34.6	206	48.8	92.5	10.10	39.7	8.4	1.3	6.80	0.93	5.51	1.18	3.21	0.44	3.61	0.50
ns4	90.41	62.08	17.30	5.98	2.21	1.27	2.12	3.93	0.95	0.20	0.09	3.7	99.93	34.2	658	15.1	36.6	6.6	24.5	211.9	17	198	20.4	5.5	136	44.2	212	57.9	111.2	12.40	44.4	8.5	1.6	6.85	1.29	7.02	1.55	3.87	0.59	4.05	0.61
ns4	93.13	64.17	16.13	5.96	2.11	1.10	1.94	3.72	0.80	0.14	0.09	3.7	99.94	13.7	602	14.2	33.2	5.0	24.2	193.5	15	195	17.5	4.8	116	37.7	167	47.7	92.7	10.64	40.2	8.5	1.6	6.46	1.05	6.35	1.26	3.41	0.48	3.41	0.58
ns4	95.27	61.16	18.00	6.20	2.15	1.06	1.52	4.30	0.84	0.15	0.07	4.4	99.92	13.7	593	12.5	33.3	4.8	21.9	247.4	17	202	18.7	5.2	139	43.5	170	47.6	94.8	10.74	41.1	8.4	1.5	7.59	1.17	7.21	1.55	3.96	0.58	4.11	0.68
ns4	95.80	59.91	19.50	5.39	2.14	1.01	1.37	4.85	0.75	0.15	0.06	4.7	99.91	30.8	632	11.5	38.7	5.0	18.4	301.0	19	239	21.1	6.6	156	41.9	168	39.9	78.9	9.45	36.6	7.2	1.3	6.38	1.13	6.60	1.46	4.01	0.63	4.27	0.64
ns4	97.11	65.13	15.61	5.91	1.94	1.19	1.70	3.60	0.80	0.20	0.08	3.7	99.93	30.8	528	14.2	32.2	5.8	22.6	189.2	14	188	17.9	5.3	112	40.5	199	45.3	88.7	10.14	42.0	8.1	1.5	7.24	1.20	7.04	1.32	3.92	0.56	3.62	0.62
ns4	98.08	64.53	16.18	4.91	1.77	1.41	2.05	3.85	0.89	0.18	0.06	4.0	99.91	23.9	643	13.0	54.3	8.7	19.3	207.0	16	297	23.1	7.3	115	48.9	291	55.2	110.0	12.98	51.7	11.1	1.7	8.00	1.34	8.40	1.62	4.48	0.61	4.33	0.71
ns4	98.84	67.88	14.18	5.49	1.70	1.16	2.09	3.10	0.75	0.17	0.07	3.3	99.96	27.4	513	12.5	31.4	6.5	23.4	158.2	12	211	18.1	4.5	91	41.1	204	45.8	92.6	10.87	41.2	9.9	1.6	7.84	1.11	7.50	1.41	3.82	0.57	3.72	0.55
ns4	100.01	58.21	19.49	6.72	2.33	1.02	1.40	4.74	0.71	0.13	0.08	5.0	99.92	27.4	670	17.2	42.5	5.1	21.9	272.9	18	255	22.1	5.2	131	35.6	153	40.2	84.1	9.61	35.7	8.6	1.3	6.80	1.10	6.13	1.29	3.31	0.49	3.30	0.50
ns4	101.01	57.01	20.36	6.55	2.47	1.18	1.65	4.85	0.64	0.11	0.08	4.9	99.89	17.1	653	11.4	40.0	4.5	19.5	272.4	16	352	29.7	3.9	117	33.8	144	57.9	106.1	11.86	41.6	8.3	1.2	5.86	0.90	5.73	1.15	3.00	0.43	2.81	0.47
ns4	102.02	65.37	15.40	5.88	1.92	1.20	1.89	3.52	0.65	0.26	0.08	3.6	99.84	13.7	558	11.8	25.1	5.2	21.9	191.1	13	239	16.4	6.0	98	39.9	170	44.8	87.1	10.35	41.9	8.4	1.4	7.33	1.00	6.39	1.30	3.50	0.46	3.34	0.54
ns4	103.14	64.82	15.91	5.58	1.99	1.22	2.14	3.75	0.78	0.19	0.08	3.3	99.85	13.7	682	12.6	30.1	5.4	19.0	189.4	13	243	16.7	4.3	109	35.7	176	43.5	83.5	10.05	41.3	7.4	1.3	5.94	1.08	5.92	1.29	3.44	0.58	3.37	0.54
ns4	104.11	62.69	16.91	5.92	2.15	1.13	1.91	4.09	0.73	0.17	0.08	4.0	99.87	6.8	690	13.4	31.7	4.6	20.5	226.0	14	269	16.0	4.5	117	33.8	153	43.4	80.3	9.95	41.5	7.5	1.3	5.70	0.95	5.72	1.17	3.40	0.53	3.08	0.49
ns4	104.96	59.71	18.98	5.96	2.43	0.95	1.41	4.96	0.74	0.14	0.08	4.5	99.95	23.9	680	10.9	38.2	4.1	20.2	310.5	17	236	17.8	5.0	157	33.1	131	33.6	66.1	8.04	36.6	6.3	1.3	5.41	0.91	5.45	1.07	3.28	0.51	3.30	0.52
ns4	105.92	60.43	18.05	7.10	2.46	0.94	1.49	4.35	0.70	0.13	0.09	4.1	99.93	10.3	673	17.0	36.5	4.6	23.2	274.7	15	265	17.6	4.2	135	30.8	132	42.8	79.0	9.46	37.8	7.2	1.3	5.78	0.97	5.44	1.07	2.87	0.51	3.02	0.48
ns4	106.83	59.28	17.41	7.67	2.58	0.91	1.42	4.34	0.65	0.14	0.10	5.3	99.88	20.5	627	15.3	37.9	3.3	23.2	257.6	14	234	18.2	4.1	118	28.6	105	45.5	81.6	9.83	40.9	7.5	1.2	5.44	0.86	5.15	0.95	2.75	0.44	2.68	0.44
ns4	108.02	59.65	17.58	5.90	2.33	1.82	1.47	4.51	0.65	0.80	0.08	5.0	99.87	20.5	680	9.0	34.5	4.1	17.6	251.5	15	261	16.8	5.2	118	46.3	119	53.6	89.6	11.59	50.5	9.3	1.6	8.47	1.33	7.42	1.49	3.93	0.63	3.58	0.55
ns4	110.11	66.08	15.16	5.15	2.00	1.20	2.33	3.40	0.67	0.18	0.08	3.5	99.84	13.7	715	11.3	23.5	4.5	17.9	162.6	10	331	14.6	4.8	86	30.2	161	42.9	77.3	9.14	35.6	5.9	1.2	5.19	0.95	5.10	0.97	2.84	0.42	2.98	0.43
ns4	112.11	68.00	14.25	4.66	1.83	1.30	2.32	3.27	0.65	0.16	0.07	3.2	99.81	17.1	729	10.4	23.7	6.4	16.0	155.2	10	361	15.3	4.1	83	30.0	189	41.6	78.4	9.16	36.6	6.1	1.2	5.24	0.87	4.91	1.01	3.11	0.47	2.66	0.40
ns4	114.24	29.63	14.23	2.10	1.34	23.4	0.50	4.22	0.26	0.05	1.10	22.9	99.78	3.4	574	4.0	1.6	6.5	1.6	235.3	5	432	43.4	9.3	14	82.9	162	47.6	70.4	8.15	33.8	6.6	1.0	7.27	1.30	8.70	2.15	7.15	1.18	7.35	1.24
ns4	115.77	54.13	22.08	6.70	2.60	0.99	1.26	5.64	0.77	0.14	0.08	5.5	99.99	23.9	807	18.6	41.3	5.0	26.0	361.2	20	241	22.6	5.8	161	40.7	162	43.2	81.4	9.60	38.7	7.0	1.2	6.76	1.17	6.83	1.40	4.30	0.64	4.15	0.61
ns4	119.18	58.79	19.02	6.04	2.25	1.22	2.04	4.69	0.89	0.18	0.09	4.6	99.92	23.9	827	12.6	29.5	6.5	21.3	252.9	15	211	20.9	5.0	127	42.1	201	50.3	94.2	11.36	43.7	8.6	1.4	7.28	1.26	7.47	1.40	4.29	0.72	3.95	0.62
ns4	127.70	50.36	24.66	6.99	2.87	1.11	1.03	6.53	0.91	0.14	0.09	5.3	100.09	34.2	775	12.2	49.9	5.4	23.7	384.6	22	185	23.0	5.8	181	40.8	166	42.7	80.0	9.91	40.3	7.6	1.4	6.99	1.23	7.37	1.50	4.31	0.68	4.33	0.74
ns4	130.69	54.99	21.53	6.18	2.55	1.22	1.66	5.51	0.96	0.19	0.08	5.0	99.98	30.8	803	11.8	38.7	5.8	21.5	302.5	20	183	21.4	6.5	137	41.5	187	49.2	93.0	10.96	42.6	8.2	1.5	6.48	1.28	7.56	1.50	4.20	0.66	4.23	0.65
ns4	135.88	61.07	17.54	5.76	2.10	1.28	2.30	4.32	0.93	0.19	0.08	4.2	99.88	20.5	843	13.8	45.6	7.3	22.7	212.1	14	210	20.4	5.3	112	43.4	247	53.3	100.4	12.02	48.9	8.6	1.6	7.59	1.35	7.42	1.44	4.21	0.76	3.96	0.64
ns4	138.00	62.74	16.12	5.50	1.89	1.25	2.39	3.87	0.89	0.20	0.08	4.8	99.83	20.5	829	14.6	66.4	7.8	23.7	172.9	13	202	19.9	5.8	112	39.3	261	52.4	98.8	11.52	42.8	8.2	1.6	7.31	1.27	6.92	1.39	3.92	0.69	4.12	0.65
ns4	143.65	64.44	14.97	5.37	1.57	1.17	2.92	3.28	0.74	0.18	0.08	5.0	99.82	30.8	792	13.4	58.0	9.3	20.0	140.9	14	208	17.1	4.9	119	39.4	303	47.2	92.9	11.07	43.0	7.9	1.6	7.43	1.26	7.33	1.33	4.00	0.59	3.77	0.56
ns4	146.76	54.52	21.76	7.18	2.74	1.05	1.21	5.33	0.86	0.15	0.09	5.0	100.00	44.5	710	12.3	40.9	4.1	24.0	302.0	21	159	20.0	7.4	167	36.4	145	41.9	80.6	9.56	34.9	7.4	1.3	5.93	0.99	5.71	1.13	3.62	0.63	3.45	0.60
ns4	147.89	56.52	19.70	8.24	2.66	0.88	0.84	4.85	0.74	0.12	0.10	5.2	99.93	30.8	633	14.3	46.6	3.5	28.2	277.3	18	133	19.8	4.2	137	33.4	119	42.6	80.8	9.82	38.1	6.9	1.3	6.13	0.95	5.71	1.16	3.36	0.51	2.87	0.48
ns4	149.00	60.68	17.45	7.67	2.51	0.94	1.10	4.24	0.78	0.14	0.09	4.2	99.88	23.9	575	37.8	35.8	3.8	48.7	225.7	16	115	17.3	4.7	123	32.5	119	40.6	76.9	9.37	36.9	6.7	1.4	6.24	1.04	5.44	1.15	3.25	0.51	3.29	0.45
ns4	150.01	59.47	18.43	7.21	2.48	0.96	1.20	4.64	0.80	0.14	0.09	4.4	99.91	27.4	637	15.9	34.6	4.0	29.6	253.8	16	131	19.8	4.4	129	34.6	132	43.2	83.3	9.99	38.0	7.6	1.5	6.69	1.18	6.16	1.14	3.24	0.52	3.29	0.44
ns4	151.03	58.31	19.71	6.55	2.54	0.99	1.19	5.04	0.84	0.13	0.08	4.5	99.97	27.4	679	13.7	32.5	4.2	25.2	282.3	18	142	20.5	5.1	143	37.4	142	49.1	93.9	11.11	42.3	8.8	1.5	6.87	1.22	6.41	1.23	3.72	0.59	3.75	0.56
ns4	151.89	56.61	20.55	6.39	2.48	1.39	1.14	5.27	0.70	0.49	0.07	4.8	99.98	17.1	756	11.6	40.6	4.1	20.0	301.5	19	179	21.4	6.5	138	44.4	141	53.2	103.1	13.29	54.8	10.2	1.6	9.44	1.48	7.84	1.49	4.45	0.66	4.33	0.62
ns4	153.05	60.11	17.75	7.60	2.49	0.92	1.14	4.19	0.77	0.13	0.09	4.6	99.88	51.3	640	13.2	37.3	4.2	25.8	225.0	16	124	17.8	4.9	111	31.6	130	37.7	71.4	8.83	33.5	6.1	1.3	6.31	0.95	5.83	1.15	3.15	0.46	3.09	0.46

Core	Stratigr level	SiO2	Al2O3	Fe2O3	MgO	CaO	Na2O	K2O	TiO2	P2O5	MnO	Cr	Ba	Sc	Sr	V	Y	Zr
		%	%	%	%	%	%	%	%	%	%	ppm	ppm	ppm	ppm	ppm	ppm	ppm
ns2	4.97	65.60	15.27	4.91	1.76	1.05	2.56	3.06	0.76	0.07	0.07	57.1	574	13	113	89	37.0	234
ns2	5.80	64.80	16.12	5.68	2.04	1.05	2.36	3.35	0.80	0.08	0.08	62.2	609	15	110	102	38.1	208
ns2	7.06	57.90	18.12	6.40	2.31	1.06	2.20	3.91	0.87	0.09	0.09	69.9	651	16	103	123	38.7	202
ns2	9.26	54.80	21.97	6.86	2.58	1.05	1.09	5.67	0.85	0.07	0.07	77.5	758	21	83	142	38.5	174
ns2	9.60	59.40	18.25	6.49	2.42	1.03	1.73	4.28	0.90	0.10	0.10	85.3	682	18	85	128	39.1	181
ns2	10.30	67.10	14.90	4.99	1.71	0.95	2.77	2.92	0.67	0.09	0.09	52.8	672	11	126	84	33.3	179
ns2	18.32	54.20	21.06	6.79	2.47	1.07	1.90	5.00	0.97	0.10	0.10	83.4	754	20	118	144	41.1	214
ns2	22.07	58.40	19.54	6.82	2.44	1.11	2.15	4.47	0.97	0.11	0.11	79.4	726	19	130	146	41.5	205
ns2	23.11	60.30	18.04	6.05	2.25	1.01	1.82	4.37	0.87	0.09	0.09	66.4	668	17	121	123	38.8	175
ns2	23.90	55.70	19.77	6.11	2.39	1.03	1.47	5.02	0.96	0.09	0.09	83.8	693	20	126	148	40.1	185
ns2	24.96	61.20	17.48	6.24	2.18	0.94	1.77	4.19	0.82	0.09	0.09	60.4	673	16	126	118	38.3	164
ns2	25.79	60.60	18.01	5.85	2.17	0.77	1.49	4.51	0.75	0.08	0.08	67.8	636	16	99	116	29.5	135
ns2	26.66	61.50	18.72	6.39	2.27	0.95	1.53	4.60	0.88	0.09	0.09	73.2	665	18	119	129	41.4	172

Core	Stratig level	SiO2	Al2O3	Fe2O3	MgO	CaO	Na2O	K2O	TiO2	P2O5	MnO	Cr	Ba	Sc	Sr	V	Y	Zr
		%	%	%	%	%	%	%	%	%	%	ppm	ppm	ppm	ppm	ppm	ppm	ppm
ns2	27.52	60.40	19.09	6.37	2.45	1.02	1.76	4.78	0.94	0.10	0.10	77.5	709	19	139	134	39.5	181
ns2	28.46	65.60	16.44	5.96	2.01	0.96	2.13	3.67	0.83	0.09	0.09	55.7	644	14	130	110	36.5	192
ns2	29.17	61.40	18.22	6.09	2.26	0.97	1.84	4.51	0.87	0.09	0.09	74.0	692	17	140	127	37.9	171
ns2	30.01	63.30	18.35	6.18	2.24	1.01	2.01	4.43	0.88	0.10	0.10	68.0	694	17	149	123	39.3	196
ns2	31.04	65.30	17.45	6.19	2.25	1.05	2.38	3.95	0.89	0.10	0.10	69.3	649	16	138	118	42.0	209
ns2	32.10	65.20	17.38	6.18	2.15	0.96	2.22	3.93	0.83	0.10	0.10	62.1	646	16	135	117	37.6	192
ns2	33.13	64.50	17.49	6.57	2.19	1.03	2.36	3.84	0.88	0.11	0.11	63.1	652	16	143	123	41.5	215
ns2	33.95	60.20	19.18	6.47	2.46	1.11	2.17	4.55	0.99	0.11	0.11	80.6	680	19	143	139	41.4	228
ns2	35.05	60.30	19.04	6.28	2.35	1.14	2.07	4.55	1.02	0.10	0.10	75.7	666	19	151	141	43.4	229
ns2	36.05	59.70	18.70	6.34	2.41	1.06	2.03	4.52	0.96	0.11	0.11	81.2	673	19	146	140	40.1	210
ns2	37.32	61.60	17.85	6.27	2.29	1.02	2.05	4.22	0.89	0.10	0.10	68.8	677	17	143	123	39.2	184
ns2	37.95	63.80	16.96	6.04	2.11	0.94	1.83	3.96	0.78	0.09	0.09	57.1	635	15	138	117	37.1	182
ns2	38.70	61.70	18.19	6.21	2.25	0.93	1.85	4.39	0.84	0.09	0.09	61.8	667	18	143	126	39.0	173

Appendix A

	Stratigr	SiO2	Al2O3	Fe2O3	MgO	CaO	Na2O	K2O	TiO2	P2O5	MnO	Cr	Ba	Sc	Sr	V	Y	Zr					SiO2	Zr
Core	level	%	%	%	%	%	%	%	%	%	%	ppm	ppm	ppm	ppm	ppm	ppm	ppm			sand stones		%	ppm
ns2	40.06	60.40	18.32	6.16	2.35	0.96	1.99	4.42	0.85	0.10	0.10	68.7	677	17	137	123	38.0	180					75.40	193.2
ns2	42.24	57.60	19.48	6.88	2.53	1.24	2.37	4.46	1.11	0.11	0.11	78.9	681	20	147	147	48.9	261					69.48	222.5
ns2	48.70	56.30	21.22	6.46	2.59	1.02	1.97	5.44	0.93	0.10	0.10	76.7	771	20	152	152	41.9	192					72.46	341.7
ns2	51.26	63.30	17.93	5.80	2.21	0.87	1.87	4.40	0.82	0.08	0.08	67.5	657	17	113	122	34.6	179					75.01	263.9
ns2	52.02	64.60	17.24	6.24	2.25	0.91	1.95	4.09	0.81	0.09	0.09	62.9	664	16	124	115	38.6	178					73.49	211.4
ns2	53.00	59.20	20.56	7.03	2.73	1.01	1.95	5.10	0.91	0.11	0.11	74.9	750	19	144	135	42.1	183					75.73	232.2
ns2	58.42	60.80	20.01	6.52	2.44	0.67	2.00	4.71	1.00	0.09	0.09	74.0	722	19	137	131	40.3	206					72.04	215.2
ns2	65.37	57.70	20.14	6.95	2.67	1.20	2.40	4.69	1.11	0.12	0.12	84.4	728	22	130	173	45.1	241					72.43	225.1
ns2	67.16	61.60	18.65	6.95	2.66	0.89	1.86	4.55	0.82	0.12	0.12	75.0	693	17	124	120	38.2	170					74.49	273.9
ns2	68.60	59.00	19.90	6.63	2.60	1.00	1.65	5.13	0.93	0.10	0.10	85.8	732	21	140	142	41.4	177					75.18	221.8
ns2	70.28	60.00	19.93	7.03	2.80	1.05	1.93	4.91	1.00	0.12	0.12	90.0	728	21	129	143	40.2	198					75.35	250.7
ns2	71.72	59.00	21.30	6.46	2.53	0.73	1.50	5.62	0.82	0.09	0.09	83.9	718	21	108	152	30.6	146					74.18	182.6
ns2	73.05	64.80	17.41	6.16	2.37	0.97	2.22	4.04	0.85	0.11	0.11	64.0	677	16	135	113	41.1	189						
ns2	73.94	62.10	17.35	6.24	2.38	0.99	2.10	4.02	0.88	0.11	0.11	72.4	660	17	129	119	36.8	176						
ns2	74.83	63.30	16.61	6.51	2.31	0.95	2.17	3.64	0.82	0.12	0.12	68.2	634	15	129	108	36.4	175						
ns2	76.08	60.90	18.33	6.26	2.46	0.84	1.92	4.49	0.84	0.10	0.10	74.5	690	18	126	126	33.6	154						
ns2	77.13	60.90	18.51	6.51	2.53	0.92	1.98	4.44	0.89	0.11	0.11	80.1	691	19	129	130	34.4	165						
ns2	78.05	60.00	20.70	6.32	2.51	0.67	1.47	5.54	0.77	0.09	0.09	76.3	718	20	115	143	27.6	132						
ns2	79.15	61.20	18.88	6.02	2.36	0.72	1.68	4.84	0.80	0.09	0.09	85.2	673	19	122	129	29.5	142						
ns2	79.75	58.30	20.56	6.94	2.56	0.69	1.22	5.52	0.67	0.09	0.09	71.8	751	19	146	130	34.6	138						
ns2	80.27	66.80	17.99	6.23	2.32	0.88	1.92	4.33	0.75	0.10	0.10	64.7	655	16	126	113	35.7	151						
ns2	81.47	63.70	19.80	6.35	2.35	1.02	1.61	4.98	0.84	0.08	0.08	67.6	707	19	135	128	42.3	157						
ns2	82.40	65.70	19.02	6.24	2.19	0.72	1.71	4.68	0.80	0.08	0.08	61.3	672	17	127	119	37.9	156						
ns2	83.56	65.50	18.77	6.51	2.24	0.73	1.72	4.57	0.83	0.09	0.09	62.3	677	16	128	117	39.7	165						
ns2	84.38	62.80	19.64	6.62	2.35	0.78	1.53	4.93	0.83	0.09	0.09	67.6	685	18	133	125	39.3	152						
ns2	85.56	65.10	18.60	6.11	2.21	0.69	1.66	4.57	0.80	0.08	0.08	62.6	661	16	125	118	36.6	151						
ns2	86.34	57.80	21.81	5.93	2.31	0.62	1.39	5.64	0.64	0.07	0.07	56.4	854	19	178	127	35.2	154						
ns2	87.07	59.40	20.76	6.29	2.32	0.64	1.67	5.11	0.59	0.08	0.08	54.3	831	18	179	122	30.8	132						
ns2	88.56	64.50	17.34	5.80	2.15	0.80	2.19	3.95	0.72	0.09	0.09	61.1	704	15	165	111	32.1	138						
ns2	89.37	61.70	19.19	5.69	2.25	0.78	1.71	4.88	0.68	0.08	0.08	61.1	768	17	175	129	31.1	140						
ns2	90.52	61.00	19.24	6.48	2.36	0.86	1.66	4.67	0.64	0.09	0.09	61.3	756	18	184	127	35.1	137						
ns2	91.30	59.90	18.76	6.70	2.50	0.66	1.50	4.84	0.64	0.09	0.09	63.1	702	17	164	129	30.1	122						
ns2	92.42	62.70	17.73	5.91	2.17	1.13	1.65	4.45	0.64	0.09	0.09	62.9	715	16	172	114	34.2	165						
ns2	93.75	57.00	22.11	6.73	2.60	0.83	1.59	5.75	0.94	0.09	0.09	84.1	763	23	151	170	40.8	192						
ns2	96.02	60.30	18.54	7.13	2.40	0.67	1.41	4.50	0.81	0.10	0.10	97.0	676	18	129	133	37.9	154						
ns2	98.12	55.80	21.97	7.76	2.63	0.52	0.99	5.66	0.74	0.09	0.09	79.7	762	21	145	156	34.7	151						
ns2	100.60	59.90	19.72	6.61	2.39	0.55	1.35	4.91	0.80	0.09	0.09	68.9	717	18	125	130	35.1	142						
ns2	110.22	62.00	19.44	6.27	2.32	0.27	1.61	4.72	0.81	0.08	0.08	67.9	691	17	118	128	35.0	145						
ns2	116.37	54.80	24.32	7.01	2.70	0.23	1.10	6.56	0.84	0.08	0.08	86.9	911	22	124	167	26.6	151						
ns2	118.89	59.40	19.66	7.09	2.47	0.30	1.99	4.41	0.87	0.10	0.10	69.9	651	17	128	127	34.1	172						
ns2	121.26	49.88	24.95	6.26	2.71	0.26	1.28	6.64	0.93	0.08	0.08	90.5	981	24	127	169	23.1	155						
ns2	123.10	61.40	19.42	6.24	2.36	0.29	1.85	4.56	0.86	0.08	0.08	71.8	661	18	128	133	32.1	155						
ns2	124.10	59.10	20.52	7.60	2.68	0.27	1.26	5.15	0.78	0.10	0.10	80.5	727	20	127	147	35.9	136						
ns2	124.95	59.60	20.40	7.69	2.70	0.29	1.34	4.97	0.78	0.10	0.10	79.8	702	19	125	143	32.0	127						
ns2	126.05	60.80	19.85	7.63	2.61	0.35	1.42	4.77	0.79	0.10	0.10	72.9	670	19	130	132	37.1	141						
ns2	127.05	60.30	19.24	8.06	2.66	0.37	1.39	4.56	0.75	0.11	0.11	75.1	638	18	125	132	29.3	126						
ns2	129.05	60.70	19.71	7.86	2.56	0.31	1.37	4.63	0.62	0.10	0.10	64.8	687	17	147	129	25.4	126						
ns2	130.04	59.70	19.29	7.85	2.53	0.29	1.22	4.65	0.66	0.10	0.10	71.6	666	18	127	133	29.5	118						
ns2	131.05	60.40	18.71	7.92	2.61	0.51	1.38	4.36	0.65	0.11	0.11	68.8	628	17	137	128	29.9	108						
ns2	131.95	63.00	18.78	6.67	2.11	0.63	2.00	3.97	0.56	0.09	0.09	51.7	667	16	188	121	28.7	140						
ns2	133.16	57.60	18.78	7.22	2.33	0.33	1.06	4.57	0.56	0.09	0.09	64.8	687	17	131	130	26.4	112						
ns2	135.05	55.80	18.11	7.80	2.55	0.43	1.34	4.15	0.65	0.11	0.11	65.1	647	17	143	128	29.5	115						
ns2	137.03	57.20	19.39	5.18	2.16	0.57	1.89	4.90	0.83	0.08	0.08	81.8	675	21	145	148	25.8	159						
ns2	137.93	61.60	16.77	5.23	1.94	0.35	2.52	3.46	0.95	0.08	0.08	67.3	494	17	141	125	30.7	220						
ns2	141.00	53.60	20.24	5.39	2.29	0.29	1.48	5.25	0.83	0.07	0.07	83.5	737	21	134	148	22.4	156						
ns2	143.73	57.20	19.43	5.80	2.30	0.30	1.77	4.74	0.88	0.08	0.08	78.9	671	20	137	154	30.9	173						
ns2	145.20	57.20	19.08	5.64	2.26	0.26	1.67	4.72	0.85	0.08	0.08	85.3	657	20	125	147	30.2	166						
ns2	146.48	57.20	18.14	7.20	2.51	0.40	1.38	4.37	0.71	0.11	0.11	68.4	608	18	132	125	30.5	125						
ns2	147.96	55.20	19.76	6.83	2.42	0.43	1.31	4.87	0.64	0.10	0.10	68.7	727	18	168	133	30.6	133						
ns2	149.13	57.30	19.00	7.18	2.32	0.52	1.81	4.02	0.58	0.11	0.11	53.1	673	17	189	122	27.6	123						
ns2	150.31	57.40	18.17	7.48	2.48	0.45	1.15	4.50	0.65	0.11	0.11	65.9	646	18	146	124	31.2	116						
ns2	151.30	55.50	19.90	6.15	2.13	1.05	1.03	4.87	0.58	0.08	0.08	61.2	818	18	206	128	59.6	144						
ns2	154.01	57.20	20.27	6.42	2.27	0.25	1.29	5.13	0.57	0.08	0.08	59.1	754	18	156	117	28.8	159						
ns2	156.95	59.60	18.15	6.26	1.95	0.31	1.89	3.80	0.55	0.08	0.08	48.0	676	15	179	113	26.4	140						
ns2	160.10	60.70	17.18	6.50	2.05	0.31	1.65	3.79	0.56	0.09	0.09	56.6	619	16	145	120	22.2	123						

parameters, e.g. chondrite normalised rare earth element patterns, remain approximately constant.

4. These changes suggest that there was an increasingly mafic contribution to the sediment with time although the increasing Zr and Hf suggest that there was a (lesser) increase in the felsic contribution. These apparently conflicting conclusions may be reconciled by acknowledging that the sediment source terrain may simply have become more igneous (e.g. less sedimentary rocks being weathered and supplying new sediment) although the progressively denuded rocks must have been predominantly mafic.
5. The decreasing CIA may be explained by either a progressively *less* intense weathering regime, possibly due to a less humid climate prevailing in the source terrain during the formation of the younger Skoorsteenberg Formation mudstones, or progressive uplift of younger unweathered material in the hinterland.
6. The uniformity of the rare earth element data in different fans suggests that there was only one landmass that contributed sediment to the mudstones. In general, there is little evidence for multiple sources of sediment into the basin from different landmasses.
7. Distinct anomalies occur in mudstones in one of the fans (4) in terms of many geochemical parameters. The anomalies have different magnitudes but seem to be traceable across the basin. The conventional sedimentological correlation is robust and statistically defendable. The cause of the anomalies is uncertain although introduction of a unique transient source of sediment may be invoked. The orientation of the axis of the fan for the anomalous case is at about 60° to the rest of the fans possibly supporting the case for a subtly different sediment source.
8. Geochemical data from mudstones from boreholes in the deep-water Permian Skoorsteenberg Formation in the Karoo Basin South Africa have demonstrated that chemostratigraphy is not an ideal approach to independent sedimentary correlation since the signals have substantial noise that is not simply related to lithology.

Acknowledgements

This work was sponsored by Stockholm University, Sweden, and Statoil, Norway. The NOMAD consortium (Statoil, Schlumberger Cambridge Research and the Universities of Delft, Liverpool and Stellenbosch) are thanked for their permission to sample core and to publish this paper from the results. We are indebted to Dr de Ville Wickens for introducing us to the geology of the field area and to Birgitta Boström for assistance with the ICP analyses at Stockholm University.

Appendix A

Results from geochemical analyses of all major and trace elements from the Skoorsteenberg Fm sedimentary rocks are shown.

References

Adelmann, D., & Fiedler, K. (1998). Origin and characteristics of Late Permian submarine fan and deltaic sediments in the Laingsburg subbasin (SW Karoo Basin, Cape Province/South Africa). *Zeitschrift Deutsche Geologische Gesellschaft*, *149*, 27–38.

Andersson, P. O. D., Johansson, Å., & Kumpulainen, R. A. (2003). Sm–Nd isotope evidence for the provenance of the Skoorsteenberg Formation, Karoo Supergroup, South Africa. *Journal of African Earth Sciences*, *36*, 173–183.

Andersson, P. O. D., & Worden, R. H. (2004). Mudstones of the Tanqua Basin, South Africa: an analysis of lateral and stratigraphic variations within mudstones and a comparison of mudstones within and between turbidite fans. *Sedimentology*, in press.

Armstrong, R. A., de Wit, M. J., Reid, D., York, D., & Zartman, R. (1998). Cape Town's Table Mountain reveals rapid pan-African uplift of its basement rocks. *Journal of African Earth Sciences*, *27*, 10–11.

Beckinsale, R. D., Tarney, J., Darbyshire, D. P. F., & Humm, M. J. (1977). Rb–Sr and K–Ar age determinations on samples of the Falkland plateau basement at site 330, DSDP. *Initial Reports, Deep Sea Drilling Project*, *36*, 923–927.

Bhatia, M. R. (1983). Plate tectonics and geochemical composition of sandstones. *Journal of Geology*, *91*, 611–627.

Bhatia, M. R. (1985). Rare earth element geochemistry of Australian Paleozoic greywackes and mudrocks: Provenance and tectonic control. *Sedimentary Geology*, *45*, 97–113.

Bhatia, M. R., & Crook, K. A. W. (1986). Trace element characteristics of greywackes and tectonic setting discrimination of sedimentary basins. *Contribution to Mineralogy and Petrology*, *92*, 181–193.

Blatt, H. (1980). Determination of mean sediment thickness in the crust: a sedimentological method. *Geological Society of America Bulletin*, *81*, 255–262.

Bouma, A. H., & Wickens, H. deV. (1991). Permian passive margin submarine fan complex, Karoo basin, South Africa: possible model to Gulf of Mexico. *Transactions of the Gulf Coast Association of Geological Societies*, *XLI*, 30–42.

Brown, R., Gallagher, K., & Duane, M. (1994). A quantitative assessment of the effects of magmatism on the thermal history of the Karoo sedimentary sequence. *Journal of African Earth Sciences*, *18*, 227–243.

Cole, D. I. (1992). Evolution and development of the Karoo Basin. In M. J. de Wit, & I. G. D. Ransome (Eds.), *Inversion tectonics of the Cape Fold Belt, Karoo and cretaceous basins of Southern Africa* (pp. 87–100). Rotterdam: Balkema.

Cox, R., Lowe, D. R., & Cullers, R. L. (1995). The influence of sediment recycling and basement composition on evolution of mudrock chemistry in the southwestern US. *Geochimica et Cosmochimica Acta*, *59*(14), 2919–2940.

Da Silva, L. C., Gresse, P. G., Scheepers, R., McNaughton, N. J., Hartmann, L. A., & Fletcher, I. (2000). U–Pb and Sm–Nd age constrains on the timing and source of the Pan-African Cape Granite Suite, South Africa. *Journal of African Earth Sciences*, *30*, 795–815.

Davies, S. J., & Pickering, K. T. (1999). Stratigraphic control on mudrock chemistry, Kimmeridgian Boulder Bed Succession, NE Scotland. *Chemical Geology*, *156*, 5–23.

Den Boer, L.C., (2002). *Development of a petrophysical flow model of turbidites in the Permian Tanqua sub-basin, southwestern Karoo, South Africa*. MSc Thesis. Delft University of Technology.

De Wit, M. J. (1977). The evolution of the Scotia Arc as a key to the reconstruction of southwestern Gondwanaland. *Tectonophysics*, *37*, 53–81.

Dickinson, W. R. (1974). Plate tectonics and sedimentation. In W. R. Dickinson (Ed.), *Tectonics and Sedimentation* (pp. 1–27). *SEPM Special Publications, 22*.

Duane, M. J., Welke, H. J., Allsopp, H. L., & Wilsher, W. A. (1989). U–Pb isotope systematics, ages and genesis of Karoo uranium deposits, South Africa. *South African Journal of Geology*, *92*, 49–64.

Govindaraju, K. (1989). 1989 Compilation of working values and sample description for 272 geostandards. *Geostandards Newsletter*, 13.

Hall, A. (1996). Igneous petrology. Harlow: Longman, p. 550.

Hill, I. G., Worden, R. H., & Meighan, I. G. (2000a). Geochemical evolution of a palaeolaterite: the interbasaltic formation, Northern Ireland. *Chemical Geology*, *166*, 65–84.

Hill, I. G., Worden, R. H., & Meighan, I. G. (2000b). Yttrium: the immobility–mobility transition during basaltic weathering. *Geology*, *28*, 923–926.

Hodgson, D.M., Flint, S.S., Hodgetts, D., Drinkwater, N.J., Luthi, S., Johannesson, E., (in preparation). Stratigraphic and palaeogeographic evolution of Permian submarine fan systems in the Tanqua depocentre, South Africa.

Hälbich, I. W. (1983). Geodynamics of the Cape Fold Belt in the Republic of South Africa, a summary. In N. Rast, & F. M. Delaney (Eds.), *Profiles of orogenic belts* (*vol. 10*) (pp. 21–29). *Geodynamics series*, Washington, DC: American Geophysical Union.

Hälbich, I. W. (1992). *The Cape Fold Belt—Agulhas bank Transect across the Gondwana Suture in Southern Africa. Global Geotransect 9*, Washington, DC: American Geophysical Union and Interunion Commitee on the Lithosphere, pp. 1–17.

Jarvis, I., & Jarvis, K. E. (1992a). Plasma spectrometry in the earth sciences: techniques, applications and future trends. In I. Jarvis, & K. Jarvis (Eds.), *Plasma spectrometry in the earth sciences* (*vol. 95*) (pp. 1–33). *Chemical geology*.

Jarvis, I., & Jarvis, K. E. (1992b). Inductively coupled plasma-atomic emission spectrometry in exploration geochemistry. In G. E. M. Hall (Ed.), *Geoanalysis* (*vol. 44*) (pp. 139–200). *Journal of geochemical exploration*.

Jarvis, I., Moreton, J., & Gerard, M. (1998). Chemostratigraphy of Madeira Abyssal Plain Miocene–Pleistocene turbidites, Site 950. *Proceedings Ocean Drilling Program, Scientific Results*, *157*, 535–558.

Johnson, M. R. (1991). Sandstone petrography, provenance and plate tectonic setting in Gondwana context of the southeastern Cape-Karoo Basin. *South African Journal of Geology*, *94*, 137–154.

Johnson, S. J., Flint, S., Hinds, D., & Wickens, H. deV. (2001). Anatomy, geometry and stratigraphy of basin floor to slope turbidite systems, Tanqua Karoo, South Africa. *Sedimentology*, *48*, 987–1023.

Kingsley, C. S. (1981). A composite submarine fan-delta-fluvial model for the Ecca and lower Beaufort groups of Permian age in the Eastern Cape Province, South Africa. *Transactions of the Geological Society of South Africa*, *84*, 27–40.

Marshall, J. E. A. (1994). The Falkland Islands: a key element in Gondwana paleogeography. *Tectonics*, *13*, 499–514.

Mason, B., & Moore, C. B. (1982). Principles of geochemistry. New York: Wiley, p. 344.

McLennan, S. M. (1989). Rare earth element in sedimentary rocks: influence of provenance and sedimentary processes. In B. R. Lipin, & G. A. McKay (Eds.), *Geochemistry and mineralogy of rare earth elements* (*vol. 21*) (pp. 169–200). *Reviews in mineralogy*.

McLennan, S. M., Taylor, S. R., McCulloch, M. T., & Maynard, J. B. (1990). Geochemical and Nd–Sr isotopic composition of deep-sea turbidites: crustal evolution and plate tectonic associations. *Geochimica et Cosmochimica Acta*, *54*, 2015–2050.

Mitchell, J. M., Dzerdzeevskii, B., Flohn, H., Hofmeyr, W. L., Lamb, H. H., Rao, K. N., & Walléen, C. C. (1966). *Climatic Change Technical Note No. 79*, Geneva: World Meteorological Organization, p. 79.

Morton, A. C., Todd, S. P., & Haughton, P. D. W. (1991). *Developments in provenance studies. Geological Society of London, Special Publication, 57*, p. 370.

Nesbitt, H. W. (1979). Mobility and fractionation of rare earth elements during weathering of a granodiorite. *Nature*, *279*, 206–210.

Nesbitt, H. W., MacRae, N. D., & Kronberg, B. I. (1990). Amazon deep-sea fan muds: light REE enriched products of extreme chemical weathering. *Earth and Planetary Science Letter*, *100*, 118–123.

Nesbitt, H. W., Markovics, G., & Price, R. C. (1980). Chemical processes affecting alkalis and alkaline earths during continental weathering. *Geochimica et Cosmochimica Acta*, *44*(11), 1659–1666.

Nesbitt, H. W., & Young, G. M. (1982). Early Proterozoic climates and plate motions inferred from major element chemistry of lutites. *Nature*, *299*, 715–717.

Norrish, K., & Pickering, J. G. (1983). *Clay minerals. Soils, an Australian viewpoint*, Melbourne: CSIRO, pp. 281–308.

Pearce, T. J., & Jarvis, I. (1995). High-resolution chemostratigraphy of Quaternary distal turbidites: a case study of new methods for the analysis and correlation of barren sequences. In R. E. Dunay, & E. A. Hailwood (Eds.), *Non-biostratigraphical methods of dating and correlation* (*89*) (pp. 107–143). *Geological Society of London Special Publications, 89*.

Preston, J., Hartley, A., Hole, M., Buck, S., Bond, J., Mange, M., & Still, J. (1998). Intergrated whole-rock trace element geochemistry and heavy mineral chemistry studies: aids to the correlation of continental red-bed reservoirs in the Beryl Field, UK North Sea. *Petroleum Geoscience*, *4*, 7–16.

Roser, B. P., & Korsch, R. J. (1986). Determination of tectonic setting of sandstone-mudstone suites using SiO_2 content and K_2O/Na_2O ratio. *Journal of Geology*, *94*, 635–650.

Rowsell, D. M., & De Swardt, A. M. J. (1976). Diagenesis in Cape and Karoo sediments and its bearing on their hydrocarbon potential. *Transactions of the Geological Society of South Africa*, *79*, 81–129.

Rozendaal, A., Gresse, P. G., Scheepers, R., & Le Roux, J. P. (1999). Neoproterozoic to early Cambrian crustal evolution of the Pan-African Saldania Belt, South Africa. *Precambrian Research*, *97*, 303–323.

SACS, South African Committee for Stratigraphy (1980). Stratigraphy of South Africa; Handbook 8; Part 1, Lithostratigraphy of the Republic of South Africa, South West Africa/Namibia and the republics of Bophuthatswana, Transkei and Venda. South Africa Geological Survey, Department of Mineral and Energy Affairs. Pretoria, South Africa.

Scott, E.D., (1997). *Tectonics and sedimentation: The evolution, tectonic influences and correlation of the Tanqua and Laingsburg subbasins, southwest Karoo basin, South Africa*. PhD Thesis. Louisiana State University.

Svendsen, J. B., & Hartley, N. R. (2002). Synthetic heavy mineral stratigraphy: applications and limitations. *Marine and Petroleum Geology*, *19*, 389–405.

Swan, A. R. H., & Sandilands, M. (1995). Introduction to geological data analysis. Oxford: Blackwell Science, p. 446.

Taylor, S. R., & McLennan, S. H. (1985). The continental crust: its composition and evolution. Oxford: Blackwell Scientific Publications, p. 312.

Theron, J. N. (1969). The Baviaanskloof range—a South African nappe. *Transactions of the Geological Society of South Africa*, *72*, 29–30.

Thomas, R. J., Agenbacht, A. L. D., Cornell, D. H., & Moore, J. M. (1994). The Kibaran of Southern Africa: Tectonic evolution and metallogeny. *Ore Geological Reviews*, *9*, 131–160.

Thomas, R. J., Jacobs, J., & Eglington, B. M. (2000). Geochemistry and isotopic evolution of the Mesoproterozoic Cape Meredith Complex, West Falkland. *Geological Magazine*, *137*, 537–553.

Visser, J. N. J. (1991). Geography and climatology of the late Carboniferous to Jurassic Karoo Basin in south-western Gondwana. *Annals of the South African Museum*, *99*, 415–431.

Visser, J. N. J., & Young, G. M. (1990). Major element geochemistry and paleoclimatology of the Permo-Carboniferous glacigene Dwyka Formation and post-glacial mudrocks in southern Africa. *Palaeogeography, Palaeoclimatology, Palaeoecology*, *81*, 49–57.

Vital, H., Stattegger, K., & Garbe-Schonberg, C. D. (1999). Composition and trace-element geochemistry of detrital clay and heavy-mineral

suites of the lowermost Amazon river: A provenance study. *Journal of Sedimentary Research*, *A69*, 563–575.

Wickens, H. deV., (1984). *Die stratigrafie en sedimentologie van die Groep Ecca wes van Sutherland*. MSc Thesis (unpublished). University of Port Elisabeth, South Africa. 86p.

Wickens, H. deV. (1992). Submarine fans of the Permian Ecca Group in the SW Karoo basin: Their origin and reflection on the tectonic evolution of the basin and its source areas. In M. J. de Wit, & I. G. D. Ransome (Eds.), *Inversion tectonics of the Cape Fold Belt, Karoo and Cretaceous Basins of Southern Africa, Balkema, Rotterdam* (pp. 117–125).

Wickens, H. DeV., (1994). *Basin floor fan building turbidites of southwestern Karoo Basin, Permian Ecca Group, South Africa*. PhD Thesis (unpublished). University of Port Elisabeth, South Africa. p. 233.

Wyllie, P. J. (1977). Crustal anatexis: an experimental review. *Tectonophysics*, *43*, 41–71.